2012

Studies of T-0632 interactions with GLP-1R: Synthesis of a photolabile analog

Erika Buckle
Wellesley College, ebuckle@wellesley.edu

Studies of T-0632 interactions with GLP-1R: Synthesis of a photolabile analog

Erika Buckle

Dr. David R. Haines, Advisor

Department of Chemistry

A Thesis Submitted in Partial Fulfillment of the Requirement for the Bachelor of Arts Degree with Honors in Chemistry at Wellesley College

Spring 2012

Acknowledgements

Professor Haines: It is clear that you have a passion for teaching, and it causes your students to have a passion for learning. You have taught me how to think about chemistry, and without your encouragement, I might not have considered graduate school, which I now know is the right choice for me. You have been a great mentor, and I would like to thank you for all of your help and support over the past three years.

Professor Virgo: I took my first chemistry class at Wellesley with you first year, and it was the first time that I enjoyed chemistry. You introduced it in a way that was understandable and interesting, and it was my experience in your class that encouraged me to pursue chemistry.

Professor Vardar-Ulu: You have taught me that there is more to chemistry than I thought. Chemistry impacts everyday life, and this is why it is so exciting and important. Thank you for introducing me to the exciting side of science!

The Haines Lab: I don't know where I would be without you all. We have made some great friendships, and these have kept me going when lab-work has been tough. Thank you for your encouragement, understanding, and company.

My Family: When I decided that I wanted to be a chemist, you were nothing but supportive. Thank you for encouraging me to always be the best that I can be, and for supporting me in all of my choices.

My Friends: Thank you for always being there when I needed someone to talk to. You are wonderful people, and I will miss you all.

Table of Contents

Abstract

The small, non-peptidic molecule T-0632 inhibits glucagon-like peptide-1 receptor (GLP-1R), requiring many of the same amino acids to bind as does the natural substrate, GLP-1. Therefore, we can use T-0632 to elucidate the structure of the GLP-1R binding pocket; covalent attachment of T-0632 to the binding site would provide information about the orientation and proximities of amino acids in the binding pocket. We will present the design and synthesis of an aryl azide analog of T-0632, which may act as a photoactive ligand of GLP-1R. Upon photolysis of the azido-T-0632 bound to GLP-1R, the azide moiety will generate a highly reactive nitrene, which will bind to the proximate amino acids. Analysis of the resulting modified protein may indicate the specific proximities of amino acids within the binding site which are bound to T-0632.

Introduction

Type II diabetes mellitus

Type II diabetes mellitus is currently one of the most widespread diseases in the United States, with 23.6 million people affected.[1] Complications from diabetes are not only among the leading causes of death in the United States, but other diseases such as heart disease, stroke, kidney disease, and nervous system damage are also linked to diabetes.[1]

Type II diabetes is a chronic disease that affects the metabolism of glucose.[2] In healthy people, insulin is secreted into the bloodstream from the pancreas after food consumption. The insulin allows for the transport of sugar out of the bloodstream and into the cells.[2] As the amount of sugar in the bloodstream decreases, the amount of insulin being secreted also decreases, an important feedback loop.[2]

In type II diabetes, the β-cells in the pancreas produce decreasing amounts of insulin despite high blood glucose levels, while the individual may also become resistant to the insulin produced. As a result, glucose builds up in the bloodstream instead of being absorbed into the cells; this condition is known as hyperglycemia.[2] Hyperglycemia harms the β-cells, and, as a result, the β-cells are no longer able to secrete insulin in response to high levels of glucose in the blood. Hyperglycemia has also been shown to induce apoptosis in β-cells, which worsens the symptoms as well as causes the disease to advance.[3]

There are currently many drug options for those with type II diabetes, but most are inadequate; they merely treat the effects of the disease and often have dangerous side effects such as hypoglycemia, weight gain, and edema.[4] In order to learn how to treat the causes of the disease and not just the symptoms, attention has been focused on the insulin induction pathway (Figure 1).

The insulin induction pathway

The insulin induction pathway begins with the ingestion of food. Food intake triggers the secretion of glucagon-like peptide-1 (GLP-1), a hormone secreted from the enteroendocrine L-cells.[5] The GLP-1 receptors (GLP-1R) are expressed on the cell membranes of β-cells located in the pancreas.[5] When GLP-1 binds to its receptor, cAMP is released, which induces the secretion of insulin from the β-cells.[5] Insulin is a protein hormone, and its receptor, a tyrosine kinase, is embedded in the plasma membrane of cells and is composed of two α subunits and two β subunits.[6] The α subunits are extracellular and incorporate the insulin binding site, while the β subunits are intracellular. Once insulin binds to the receptor, the α subunits induce a reaction in the β subunits; the β subunits become phosphorylated and activate the receptor.[6] The activation of the receptor triggers a cascade, in which a series of phosphorylations induces a response, namely the uptake of glucose into the cell. In

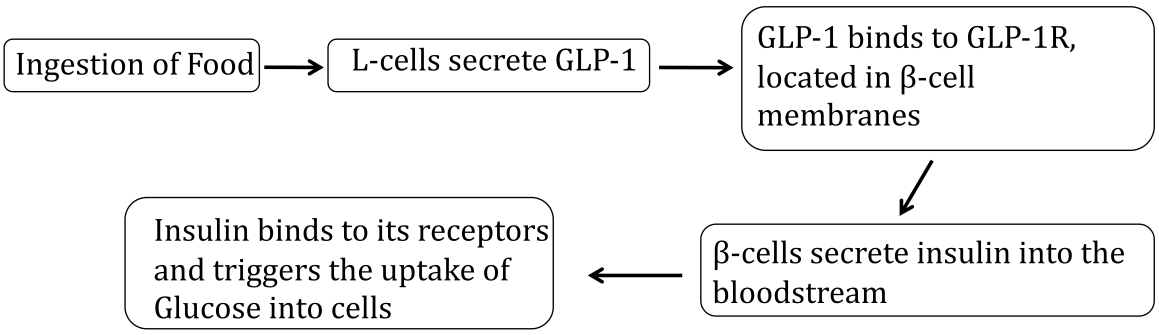

Figure 1: The insulin induction pathway.[5,6]

patients with type II diabetes, GLP-1 stimulated insulin secretion is decreased. However, the effects of the secreted GLP-1 on lowering glucose levels are still preserved.[7]

Structure and Activity of GLP-1 and GLP-1R

Understanding the insulin induction pathway does not end with knowing the sequence of events; the molecular structures of GLP-1 and its receptor as well as the interactions between them must be understood. The structure of GLP-1 is known, however its interaction with GLP-1R is not fully understood since the complete tertiary structure of GLP-1R is unknown. GLP-1R is a G protein coupled receptor belonging to the B1 Family.[8] Since it belongs to this group of receptors, a few major structural characteristics are known (Figure 2). All G protein coupled receptors have seven transmembrane helices, an extracellular N-terminus, and an intracellular C-terminus. The ligand, GLP-1, binds with the extracellular N-terminus, and the G protein coupling and signaling occur via the intracellular C-terminus.[8] The tertiary

structure of the binding domain of GLP-1R has not yet been fully determined, and the amino acids essential to binding have not all been elucidated.

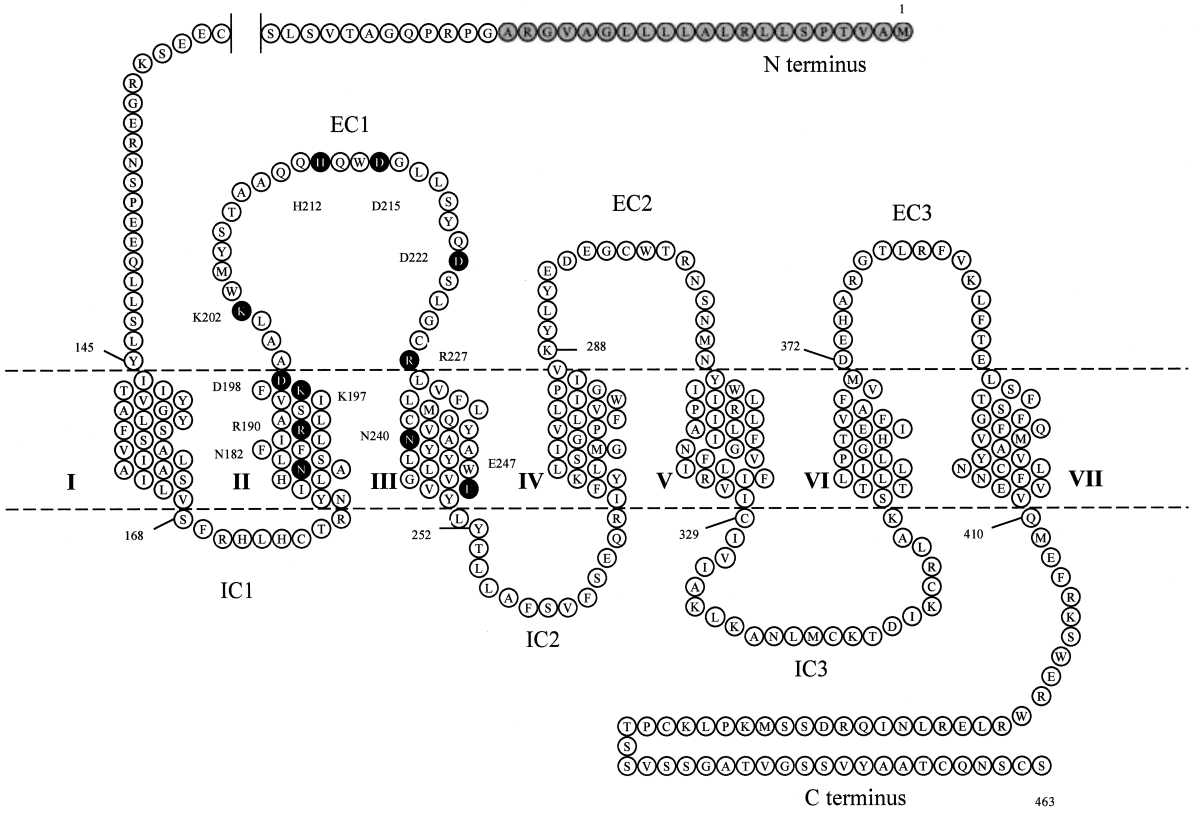

Figure 2: The predicted secondary structure of GLP-1R. The receptor contains an N-terminus, three extracellular loops (EC), three intracellular loops (IC), seven transmembrane helices, and a C-terminus. Adapted from Xiao, et al.[9]

GLP-1 is a peptide composed of 30 amino acids and is a derivative of proglucagon.[5] In the pancreas, there is post-translational processing of proglucagon, which produces an inactive pro-GLP-1, as well as other proteins. Pro-GLP-1 is then cleaved and C-terminally truncated to form the active GLP-1.[5] It is this active GLP-1 (7-36) amide that is secreted from the L cells upon ingestion of food.[5] The entire amino acid sequence of GLP-1 has been determined, but since the binding site of the

receptor has not yet been elucidated, only some structural features of GLP-1 have been shown to play an important role in binding.[10] The structure-activity relationship studies between GLP-1 and GLP-1R have shown that the N-terminal histidine is crucial for receptor affinity and the C-terminus also plays an important role in receptor interaction and recognition.[10] The spatial arrangement of GLP-1 in GLP-1R has also been predicted (Figure 3); the seven transmembrane helices

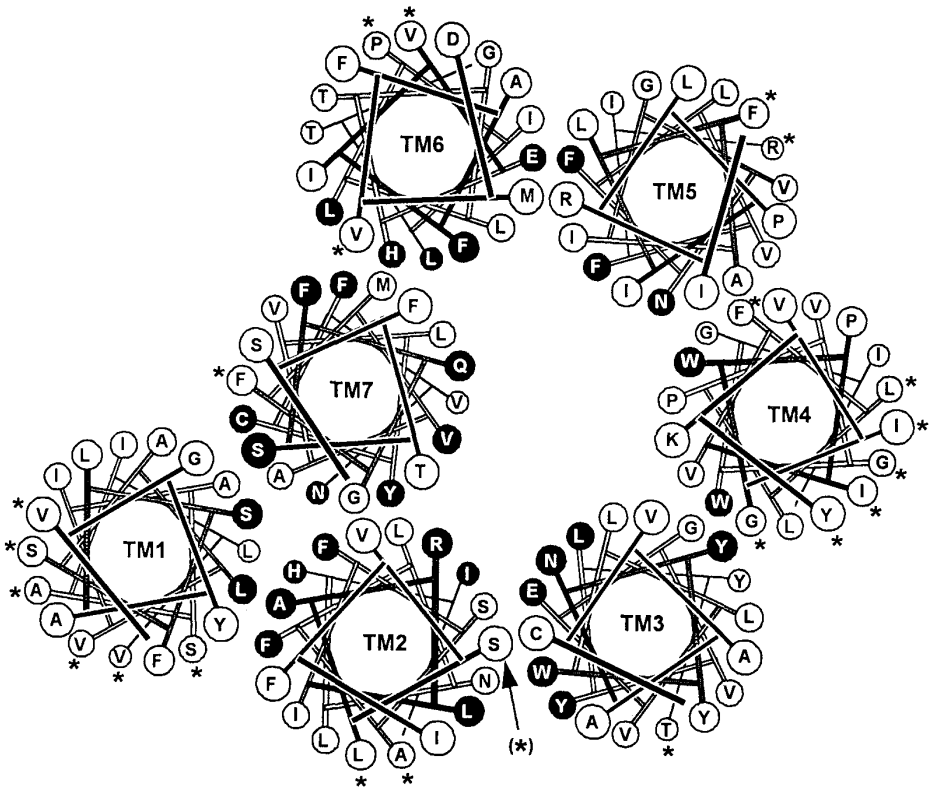

Figure 3: Arrangement of the transmembrane helices (TM) of GLP-1R. The predicted binding domain for GLP-1 is located in the center of the ring. Adapted from Donnelly, et al.[11]

are arranged counterclockwise, leaving a hollow space in the center. This space is the receptor core, which is predicted to interact with the amino-terminus of GLP-1 in the binding process.[11,12]

The N-terminal tail of GLP-1R is also essential for binding.[11] The amino-terminus of GLP-1R contains three potential sites for N-linked glycosylation, and it has been shown that N-linked glycosylation of GLP-1R is essential for the binding of GLP-1; glycosylation is important for the folding of GLP-1R and its placement in the cell membrane.[13] When glycosylation was inhibited, binding of GLP-1 did not occur.[13] NMR has shown that residues 7-30 of GLP-1 are predominantly helical in structure, and it is this carboxyl-terminal region that interacts with the amino-terminal region of GLP-1R.[12] NMR and crystal structures for segments of the isolated, ligand-bound amino-terminus of GLP-1R showed that the carboxyl-terminus of GLP-1 docks within a binding cleft of the amino-terminus of GLP-1R.[14] However, no information about the mode of docking is provided from these studies.[14]

With the increase in knowledge of the insulin induction pathway and the structures of GLP-1 and GLP-1R, new incretin-based treatments are currently being developed and used. These treatments not only treat the disease but also help prevent the disease, target its progression, and reduce the risk of complications.[4] These incretin-based treatments fall into two main categories: incretin mimetics and incretin enhancers.[4] Glucagon-like peptide-1 analogs fall into the first category, incretin mimetics.[4]

GLP-1 as a potential treatment for type II diabetes

The hormone GLP-1 performs a vital role in the release of insulin into the

bloodstream. GLP-1 lowers blood glucose levels by increasing insulin secretion as well as increasing β-cell mass, both crucially important tasks in the treatment of type II diabetes[7]. GLP-1 suppresses the secretion of glucagon during hyperglycemia but not hypoglycemia, also acting to control blood glucose levels.[7] In addition to controlling blood glucose, GLP-1 has other effects that benefit diabetics: GLP-1 delays gastric emptying and increases satiety, which can lead to weight loss (Figure 4).

Organ System		**Effects of GLP-1**
Brain		increased satiety; decreased food intake; weight loss
Stomach		decreased gastric emptying
Pancreas	α cells	decreased glucagon secretion
	β cells	increased glucose sensitivity; increased insulin secretion; increased insulin biosynthesis; increased β cell proliferation and survival

Figure 4: The positive effects of GLP-1 on various organ systems in the body.

There has been a series of studies that have documented these beneficial effects of GLP-1 as a treatment for type II diabetes. According to Chia, et al., overnight intravenous infusion of GLP-1 in patients with type II diabetes lowered fasting and post-meal glucose levels to nearly normal as well as improved β-cell function.[7] The long term results of GLP-1 treatment were also examined; patients were given GLP-1 infusions for six and twelve weeks, resulting in an obvious improvement of β-cell function and insulin sensitivity.[7] The data gathered from these studies indicate that GLP-1 treatments target the causes of type II diabetes, not only the symptoms.

However, despite these benefits, since GLP-1 has an extremely short half-life of two minutes in the bloodstream, it cannot be considered an effective treatment for type II diabetes. Once in the bloodstream, GLP-1 is degraded by the enzyme dipeptidyl peptidase IV (DPP-IV) and neutral endopeptidase (NEP) 24.11. DPP-IV cleaves the histidine-alanine head of GLP-1 *in vivo* (Figure 5). Since the N-terminal

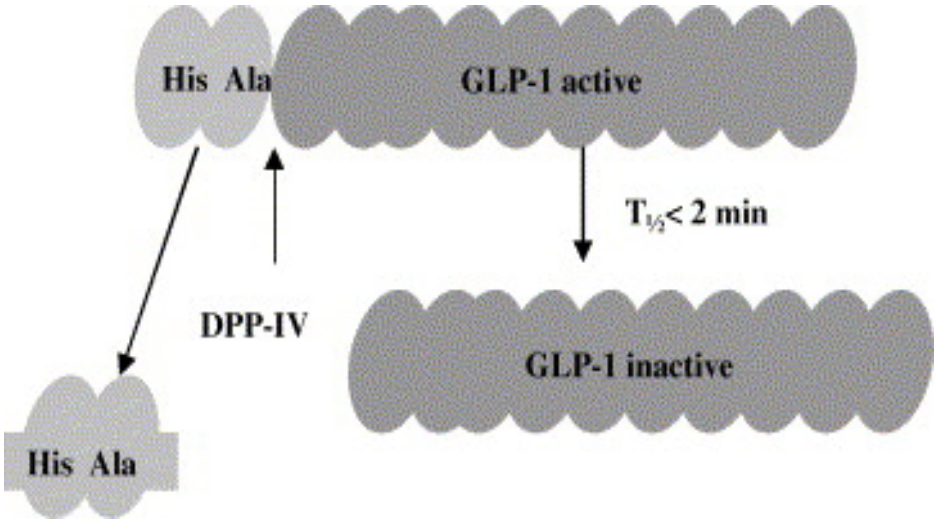

Figure 5: The inactivation of GLP-1 *in vivo* by DPP-IV. Adapted from Arulmozhi, et al.[15]

histidine is crucial for receptor interaction, this cleavage by DPP-IV renders GLP-1 inactive.[7,15] NEP 24.11 cleaves GLP-1 at six potential sites, which also renders GLP-1 inactive.[7,15] Therefore, if GLP-1 were to be considered a type II diabetes treatment, there would have to be a nearly continuous intravenous infusion of GLP-1 in patients. Despite the many benefits of GLP-1 infusion, a continuous intravenous infusion of GLP-1 in diabetic patients is impractical, so GLP-1 is not a promising drug option. Nonetheless, GLP-1 analogs, which can be designed to have an extended half-life, may be significant drug options[7].

In the past five years, GLP-1 analogs have been released as drug treatments in the United States and are delivered via injection.[16] These treatments regulate glucose levels by stimulating glucose-dependent insulin secretion and synthesis, as well as suppressing glucagon secretion, proving to be effective treatments.[16]

One such treatment is Exenatide, an approved therapy for type II diabetes patients who have not been able to achieve glycemic control with other, more conventional treatments.[7] Exenatide is the synthetic form of exendin-4 and is a 39 amino acid protein (Figure 6). It has 53% homology to GLP-1 and binds with a greater affinity to GLP-1R than does GLP-1.[7] Exenatide is not susceptible to DPP-IV

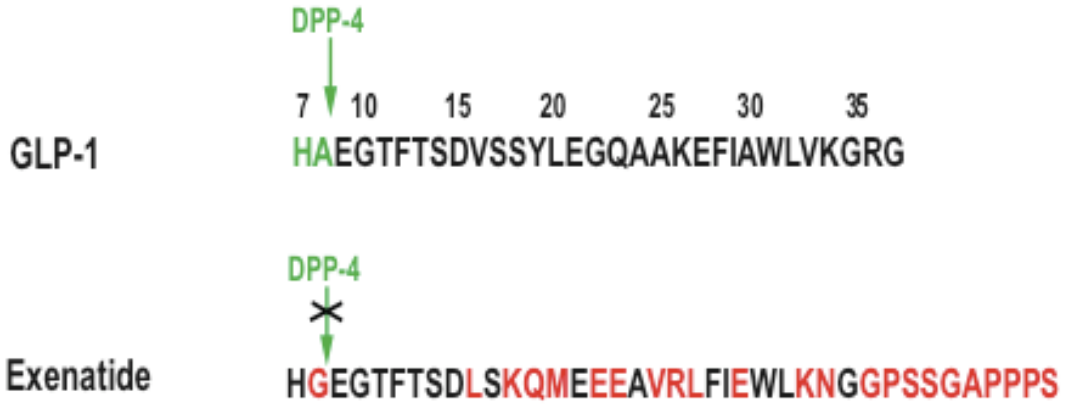

Figure 6: The structures of GLP-1 and its analog Exenatide. Differences are highlighted in red. The susceptibilities to DPP-IV are also shown. Adapted from Chia, et al.[7]

inactivation because its second amino acid is not alanine, as is the case with GLP-1, but glycine (Figure 6). Exenatide is also less susceptible to NEP 24.11 than GLP-1, thus significantly increasing the *in vivo* half-life.[7]

Exenatide is an incretin mimetic treatment. According to Addison, et al., incretin mimetic treatments, such as these GLP-1 based treatments, may also have

potential ameliorative effects on cardiovascular health, a major concern for patients with type II diabetes.[17] However, there is a significant inconvenience: incretin-mimetic drugs require injection. Therefore, it is desirable to create another GLP-1 analog that can be delivered orally; that is, a new analog must be developed that can resist degradation in intestinal fluids. In order to design a viable GLP-1 analog, it will be useful to understand the three dimensional structure of GLP-1R.

T-0632 as a Probe into the Structure of GLP-1R

The structure of the binding site of GLP-1R is being explored through T-0632, a small, non-peptidic molecule (Figure 7) that exhibits affinity for the active site of GLP-1R. Studies have shown that T-0632 inhibits the binding of GLP-1, therefore

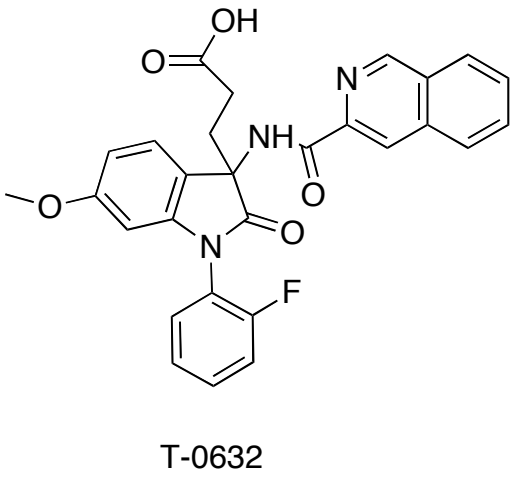

T-0632

Figure 7: The small, non-peptidic molecule T-0632.

indicating that it may bind to GLP-1R in the same location as GLP-1, interacting with many of the same amino acids. It has been shown that amino acid residue

tryptophan 33 (W33) of GLP-1R plays an important role in the binding of T-0632 (Figure 8), although it seems to be uninvolved in the binding of GLP-1.[18] There are two potential modes of interaction between W33 and T-0632 that cause T-0632 to have affinity for GLP-1R: (1) W33 interacts directly with T-0632 or (2) W33 indirectly enables T-0632 to bind to GLP-1R by causing other residues to form a binding domain.[18] In either circumstance, W33 contributes significantly and specifically to the binding of T-0632 to GLP-1R.[18] Other residues such as K288, R380, and K383 have also been shown to play a role in the binding of T-0632 to GLP-1R, though W33 seems to have the most significant role.[18,19] In order to gain more insight into how non-peptidic molecules can interact with GLP-1R, it would be useful to understand the mechanism by which T-0632 binds to GLP-1R as well as the three dimensional structure of GLP-1R.

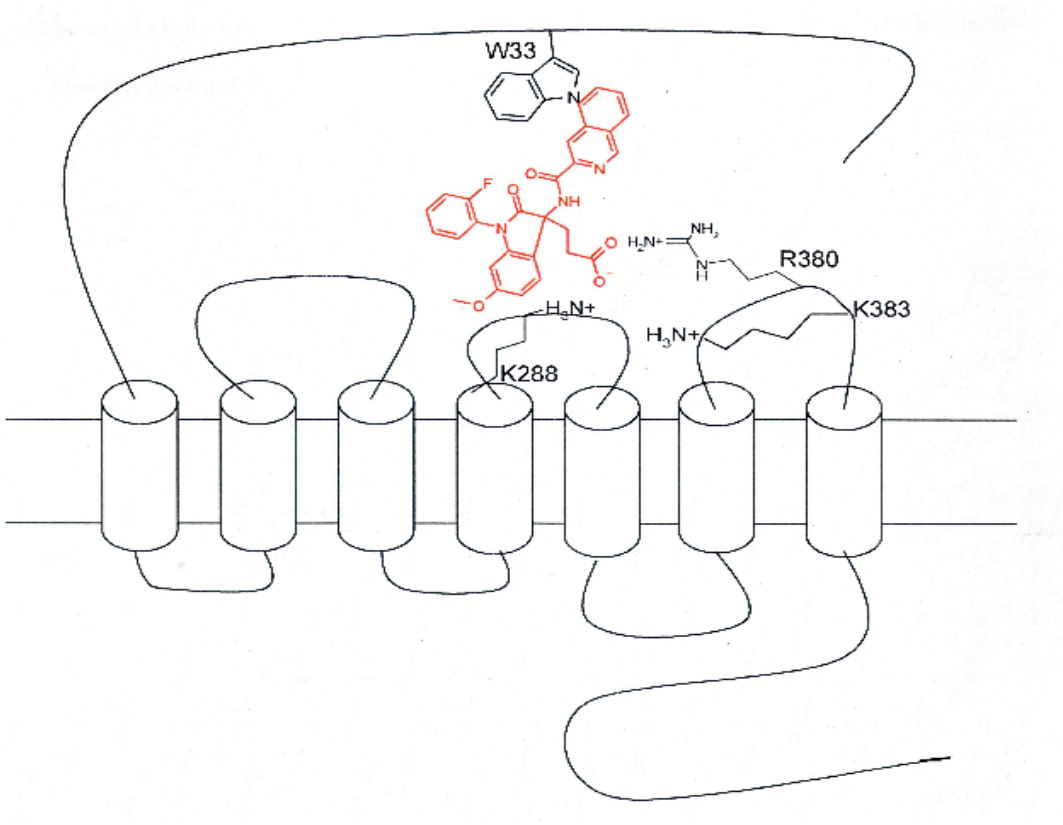

Figure 8: Interactions between GLP-1R and T-0632, in red. Adapted from Kieffer.[19]

An aryl azide analog of T-0632 (**1**) (Figure 9) is being synthesized which can be covalently bound in the GLP-1R active site, providing information about the orientation and proximities of amino acids in the binding domain. The only difference between analog **1** and T-0632 is the azide moiety. The azide moiety is a

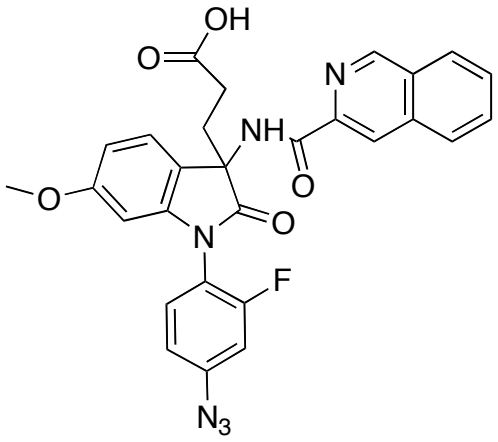

1

Figure 9: An aryl azide analog of T-0632 (**1**).

photolabile residue, and its incorporation into T-0632 allows for photoaffinity labeling. Since the azide moiety is highly reactive, it is an exceptional tool for photoaffinity labeling. Photoaffinity labeling is a process that creates a covalent bond between the ligand and an amino acid to which it is proximate in the binding domain.[20] Since G protein coupled receptors are challenging to study via direct physiochemical models due to their transmembrane structure, photolabile probes have proven to be useful.[20]

Theoretically, the process of photolabeling occurs in a few steps (Figure 10). First, the ligand binds non-covalently to the receptor. Upon exposure to ultraviolet light, the photoactive moiety on the ligand undergoes photolysis to create a highly reactive species, usually a carbene or a nitrene. The nitrene will insert non-discriminately into any covalent bond. Finally, the reactive intermediate binds irreversibly to the receptor; this covalent bond creates a label of the interaction between the ligand and the receptor.[21]

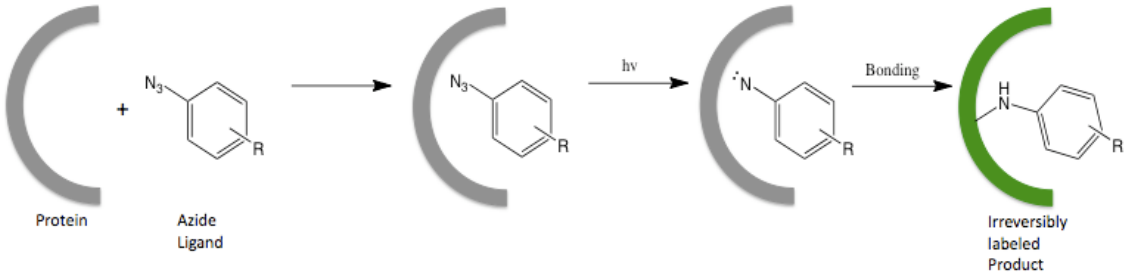

Figure 10: The process of photoaffinity labeling. Adapted from Kieffer.[19]

In this case, analog **1** is acting as the photolabile probe. Upon completion of the synthesis, we will incubate analog **1** with GLP-1R. If the fluorobenzene functional group of T-0632 interacts with GLP-1R, the azide moiety on analog **1** will allow creation of a covalent bond between **1** and GLP-1R. After incubation, the complex will be irradiated with UV radiation. The azide moiety will generate a highly reactive nitrene, which will bind to the proximate amino acids, acting as a photolabile. Analysis of the resulting modified protein will indicate the specific proximities of amino acids within the binding site. Several different azide T-0632 compounds may be required to effectively map the three-dimensional binding domain.

*Synthesis of Analog **1***

A synthesis of analog **1** has been designed (Figure 11), based on the complete synthesis of T-0632.[22] Modifications of the synthesis by Kim have been made by Kieffer to accommodate the placement of the azide moiety.[19,22] Our total synthetic

scheme is based on this scheme by Kieffer, but with modifications made where necessary.

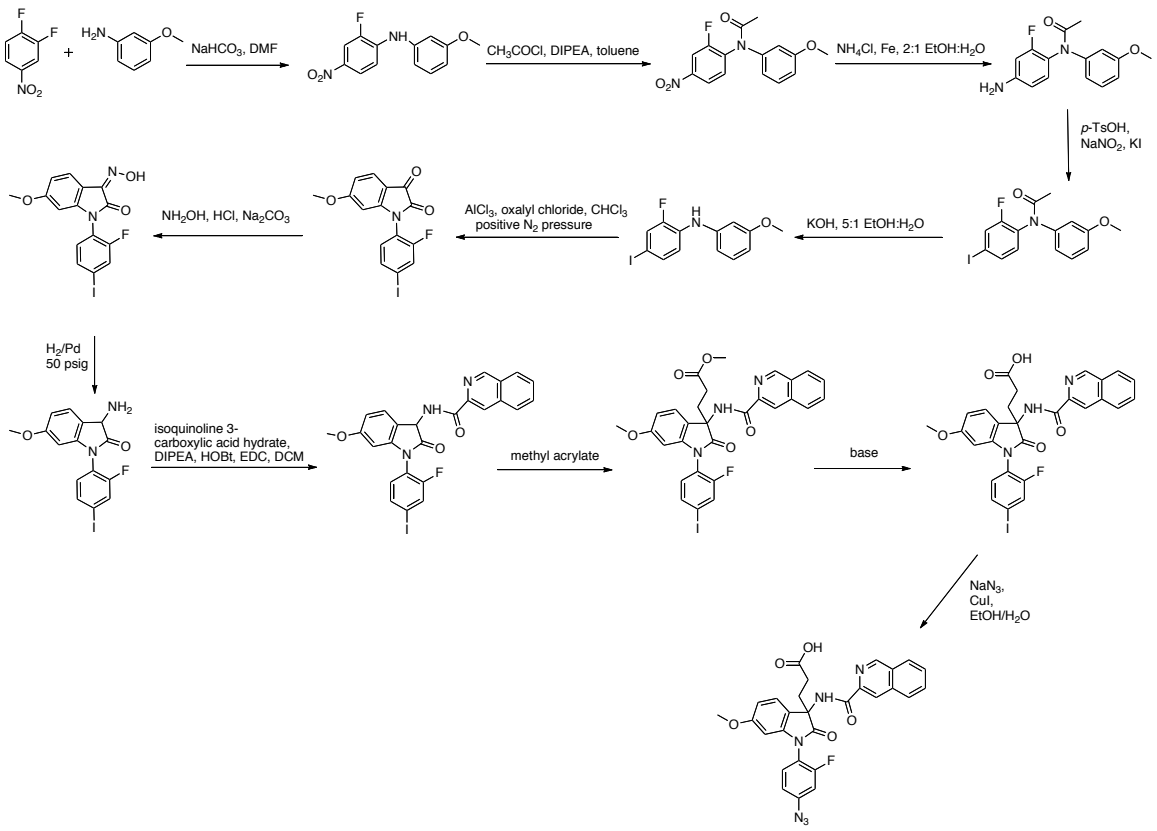

Figure 11: Synthesis of T-0632 aryl azide analog proposed by Kieffer.[19]

It is imperative that the installation of the azide moiety be the final step of the synthesis due to the high reactivity of the azide moiety. Therefore, an iodine is used as a placeholder for the azide and is installed early in the synthesis. Obtaining the iodinated acetamide **7** (Figure 12) posed many problems, including extensive polymerization, and thus required modifications to the scheme proposed by Kieffer, which will be discussed.

The steps leading up to the formation of isatin **9** (Figure 12) were successful and required no modification. In order to install the isoquinoline carboxylic acid moiety, reduction must occur. However, the reduction of the oxime of the isatin proved troublesome for Kieffer. Once Kieffer obtained the iodinated isatin, she decided to proceed in the reduction by first converting the isatin to an oxime. Although the oxime was easily formed, its conversion to the amine was unsuccessful, since catalytic hydrogenation cleaved the iodine.[19] Therefore, we have decided to bypass the oxime intermediate and use a reductive amination reaction. The decision to pursue this route will be discussed further, as well as the method used in this reduction.

Once the amine has been successfully obtained, the scheme proposes that isoquinoline carboxylic acid will be attached to the amino group. Methyl acrylate is then attached to the chiral carbon, and a base hydrolyzes the ester to an alcohol. In the final step, the iodine is replaced by the azide moiety, completing the synthesis of analog **1**.

The overall goal of this thesis is to proceed in the synthesis of analog **1** and optimize reaction conditions so that the synthesis can be completed and structure-activity relationship studies of the interaction between T-0632 and GLP-1R can be conducted. The results of these studies will provide the necessary information on the structure of GLP-1R, and thus advance the search for alternative drug treatments for type II diabetes mellitus.

Results and Discussion

The synthesis of analog **1** must be completed before any biological testing and structure-activity relationship studies can be completed. A total synthesis of this molecule was designed by Kieffer.[19] Significant progress was made by Kieffer, but modifications to this procedure were necessary in order to obtain yields substantial enough to continue in the synthesis. The modified scheme for the synthesis of analog **1** is shown below (Figure 12). These synthetic steps as well as all

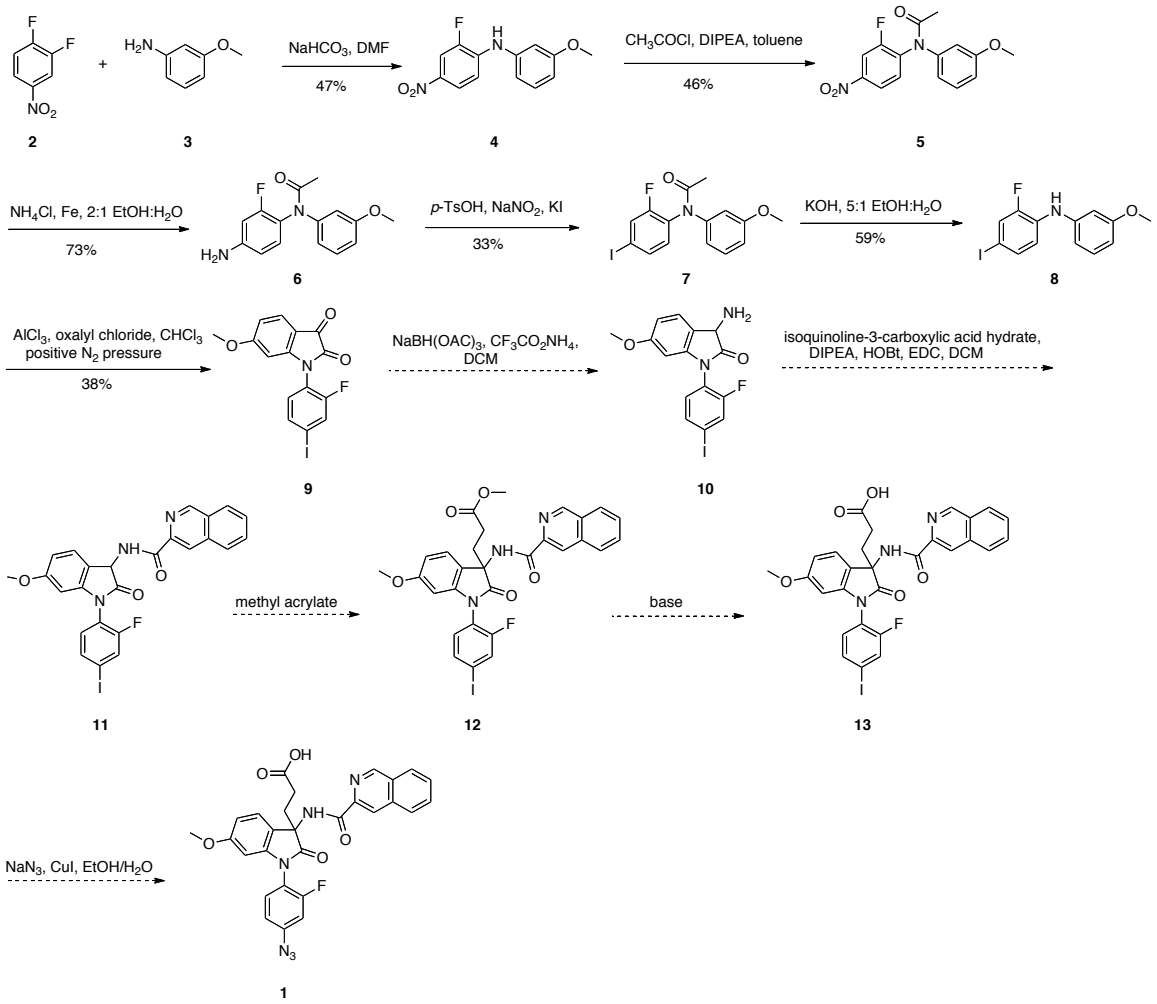

Figure 12: Proposed synthesis of **1**.

modifications made to Kieffer's scheme will be discussed.

The synthesis of analog **1** began with the production of 2-fluoro-N-(3-methoxyphenyl)-4-nitroaniline (**4**) (Figure 13). The nitro-group of the 1,2-difluoro-4-nitrobenzene (**2**) causes an ortho-para directing effect for nucleophilic aromatic substitution due to resonance. Although there are two potential leaving groups corresponding to the two fluorine atoms on the 1,2-difluoro-4-nitrobenzene,

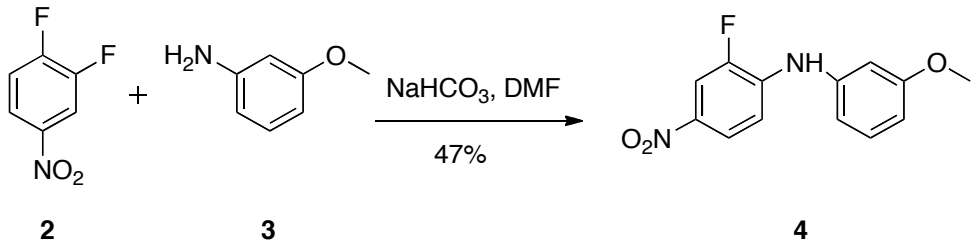

Figure 13: Formation of diphenylamine **4**.

the ortho-para directing effect causes the displacement of the fluorine in position one, para to the nitro group, only. Therefore, the production of 2-fluoro-N-(3-methoxyphenyl)-4-nitroaniline is the result of a simple nucleophilic aromatic substitution reaction (Figure 14), where the lone pair on the nitrogen attacks the para carbon. A negative charge is formed in the ring while a positive charge is formed on the nitrogen. Electrons comprising the negative charge promote the loss of the fluoride, regenerating the aromatic ring, and a proton leaves the bridging nitrogen, resulting in diphenylamine **4**.

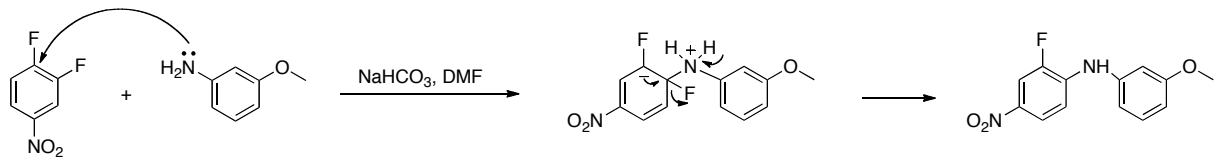

Figure 14: Mechanism of the formation of diphenylamine **4**.

The next step in the synthesis was the protection of the bridging amine in **4** with an acyl group, producing N-(2-fluoro-4-nitrophenyl)-N-(3-methoxyphenyl)acetamide (**5**) (Figure 15). In order to proceed in the synthesis, the nitro group must be reduced to an amine. However, if reduction of the nitro group occurs without protecting the bridging nitrogen, there will be two amines in the

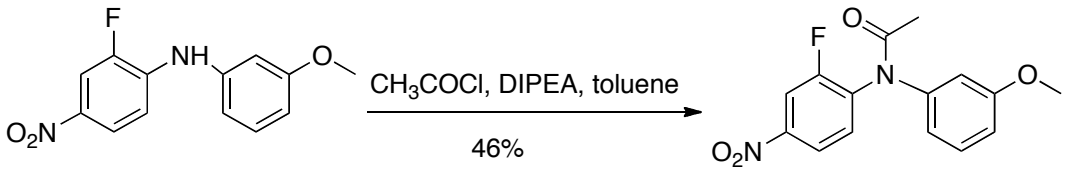

4 **5**

Figure 15: Formation of acetamide **5**.

molecule. This would prevent the selective reaction of one of the amines, leaving us with no way to selectively proceed in the synthesis. Therefore, before reduction, we must protect the only amine in **4**.

The secondary amine of **4** is a poor nucleophile, due to its proximity to two electron-withdrawing benzene groups. This lack of nucleophilicity restricts the ease with which acylation can occur. Kieffer tested a variety of conditions varying the base and electrophile, optimizing the reaction by using acetyl chloride and the sterically hindered base diisopropylethylamine (DIPEA).[19]

In this protection reaction, DIPEA deprotonates the bridging nitrogen, (Figure 16). The nitrogen then attacks the carbonyl carbon of acetyl chloride.

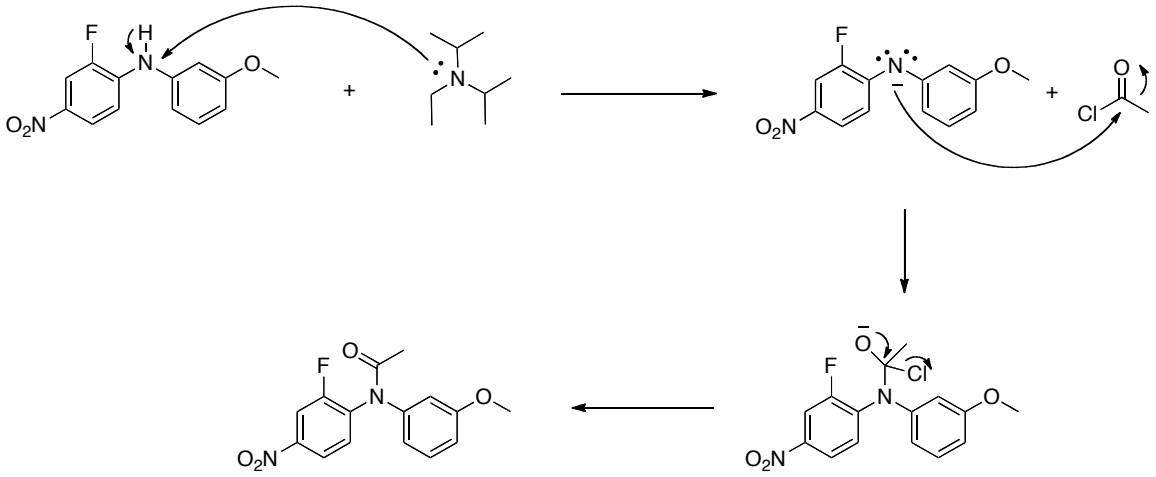

Figure 16: Mechanism of acylation of the bridging amine in **4**.

The electrons on the oxygen donate into the bond, forming a double bond and causing the chloride to act as a leaving group.

Once the acyl protecting group has been installed, we can focus on installing the iodine on the fluorobenzene. In order to replace the nitro-group with iodine, which will act as a placeholder for the azide group in the completed analog **1**, we must first reduce the nitro-group to an amine (Figure 17). This reduction was achieved by following the procedure of Renslo, et al., adapted by Kieffer.[23,19]

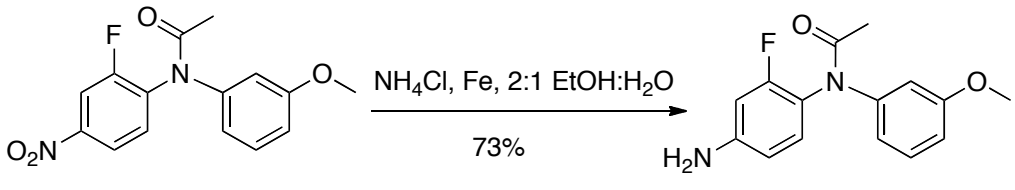

5 **6**

Figure 17: Reduction of acetamide **5**.

The exact mechanism of this reduction is not fully understood, but some inferences can be made. The mechanism involves a redox reaction revolving around the solid iron powder. The Fe^0 is oxidized to Fe^{2+}, which can then catalyze the reduction of the nitro group. The catalytic properties of the iron powder are based on surface area, so this reaction can only be conducted on a small scale. Based on what we know about the reduction, we have proposed a possible mechanism (Figure 18). The oxidized iron can form a complex with the doubly bonded oxygen

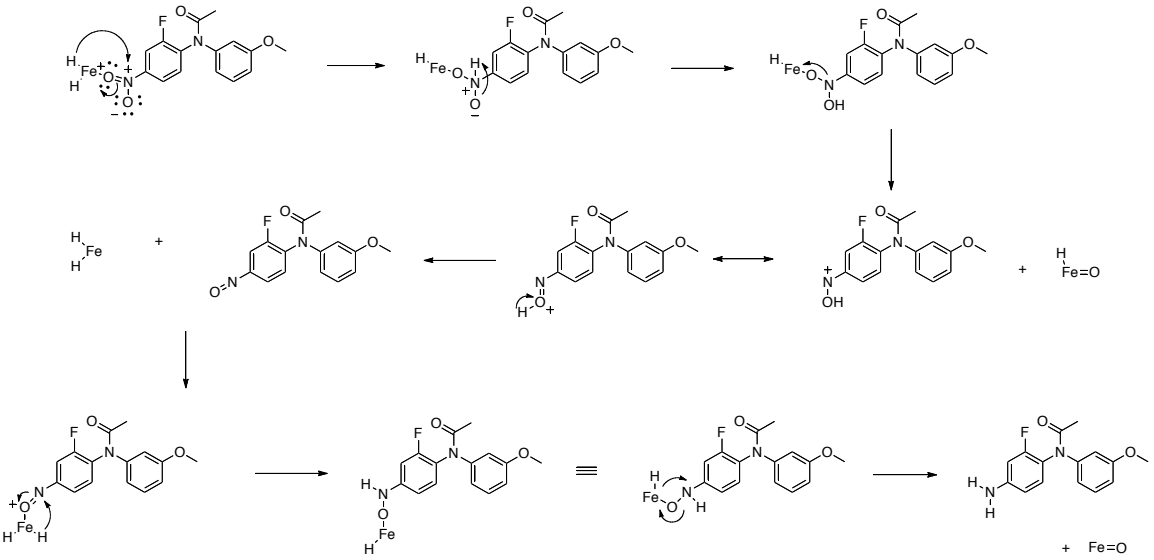

Figure 18: A proposed mechanism for the reduction of the nitro group of **5** to an amine.

of the nitro group. A hydride then donates into the nitrogen while electrons from the double bond donate into the oxygen. The proton rearranges to bond to the negatively charged oxygen, while the other oxygen leaves with the iron species. The proton will leave the oxygen, creating an N=O bond. This oxygen can then form a complex with the iron species, as seen in the first step. A hydride on the iron will donate to the nitrogen, whose double bond will donate electrons to the oxygen,

creating a nitrogen singly bonded to both a hydrogen and an oxygen. The hydride bonded to the iron will then donate into the nitrogen creating the desired amine.

This reaction proceeded in 73 % yield, but due to the tendency for the acyl protecting group to rearrange to the amino group, the resulting N-(4-amino-2-fluorophenyl)-N-(3-methoxyphenyl)acetamide (**6**) must be stored under the inert gas nitrogen and used quickly. The possibility of rearrangement discouraged column chromatography, and the product was carried on to the next step without purification.

Amine **6** was converted to N-(2-fluoro-4-iodophenyl)-N-(3-methoxyphenyl)acetamide (**7**) through a diazotization reaction and subsequent

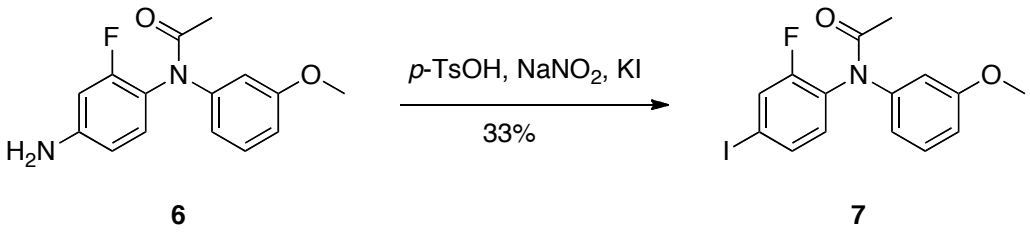

6 **7**

Figure 19: Formation of acetamide **7**.

Sandmeyer coupling (Figure 19). A nitrosonium ion is generated from *p*-toluene sulfonic acid (*p*-TsOH) and sodium nitrite ($NaNO_2$) . The nitrosonium ion attacks the aryl amine, causing nitrosation (Figure 20). Protonation of the nitrosamine and loss of water yields the diazonium ion. Potassium iodide (KI) is then added, and the iodine replaces the diazonium in a nucleophilic aromatic substitution reaction.

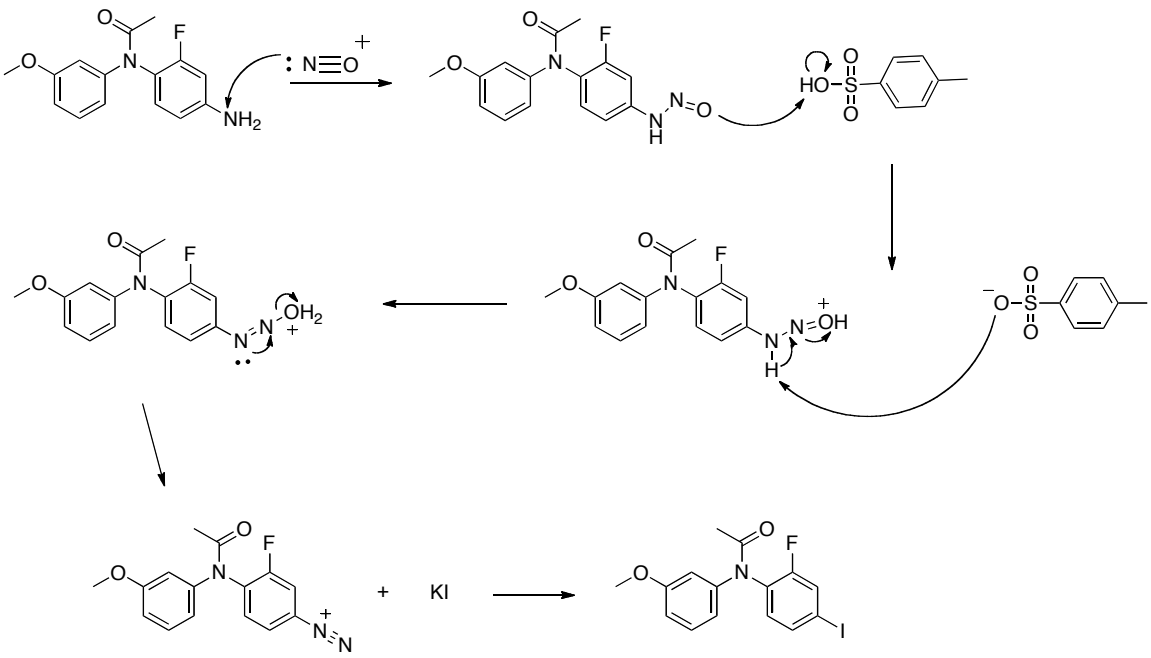

Figure 20: Diazotization and subsequent Sandmeyer reaction to produce **7**.

The diazonium ion is extremely reactive and the second aromatic ring is activated toward electrophilic aromatic substitution, both of which facilitate side-product formation, specifically dimerization and polymerization (Figure 21). In order to reduce the number of side-products, the diazotization and iodination of **6**

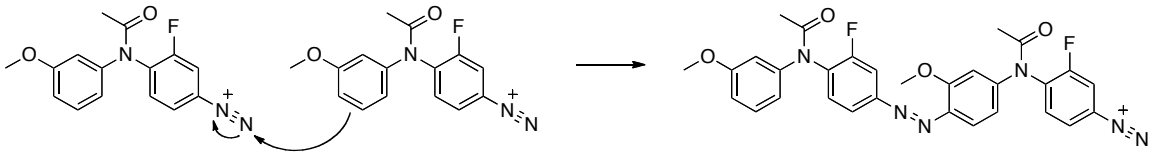

Figure 21: Side product formation during diazotization of amine **6**.

was completed in a solventless reaction described by Gorlushko, et al. and adapted by Kieffer.[24,19] However, this modification did not solve all of the problems posed by the reactivity of the diazonium ion. In an attempt to decrease side reactions, two

equivalents of silica gel were added to the mortar and pestle with the hopes of spreading out the reactive diazonium ions. However, this was not successful, resulting in no product formation. This result could be due to the polarity of the silica gel, which could interact with the intermediates, thus creating its own side-products.

The use of silica gel was abandoned, and instead, the entire reaction was conducted on ice. However, only a 17% yield was obtained with this method, a yield that is still too low for the advancement to the next step. It seemed as though there was a decrease in polymerization, but an increase in dimerization, as was observed with color differences and distinction between column chromatography results. Therefore, yet another modification is necessary in order to achieve a higher yield.

It is possible that KI is reacting with the $NaNO_2$ rather than selectively attacking the diazonium ion. Therefore, one equivalent of KI would not be sufficient to produce high yields of **7**. In order to amend this oversight, 2.5 equivalents of KI were added to the reaction mixture, which was still kept on ice. This modification increased the percent yield to 33%, enough for progression to the next step. In the future, other modifications should be made to this reaction to see if higher yields can be achieved.

Once the iodine has been inserted, there is no longer a need to protect the bridging nitrogen with an acyl group. Furthermore, deprotection needs to occur in order to proceed in the synthesis. The literature reports the use of both acids and bases to catalyze this hydrolysis reaction.[25,26] Kieffer tested a variety of conditions, varying the acid or base catalyst, and found that many conditions resulted in the

cleavage of the iodine. She optimized the reaction by using potassium hydroxide (KOH).[19]

Acetamide **7** was converted into 2-fluoro-4-iodo-N-(3-methoxyphenyl)aniline (**8**) through reaction with the strong base KOH (Figure 22).

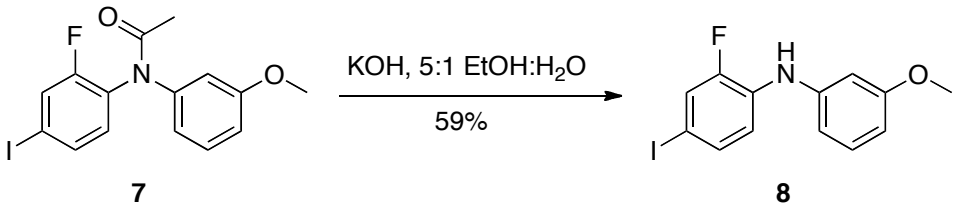

7 **8**

Figure 22: Deacylation of acetamide **7**.

Potassium hydroxide dissociates, providing a good source of OH^-, which acts as a nucleophile. The nitrogen will act as the leaving group, and the original amide will be deacylated, a result of a nucleophilic substitution reaction. This reaction mechanism produced amine **8** in 59 % yield.

Now that the protecting group has been removed, an acid chloride intermediate will be formed so that a Friedel-Crafts Acylation reaction can produce 1-(2-fluoro-4-iodophenyl)-6-methoxyindoline-2,3-dione (**9**) (Figure 23). The reaction conditions were based on the procedure of Kieffer, adapted from Kim.[19,22]

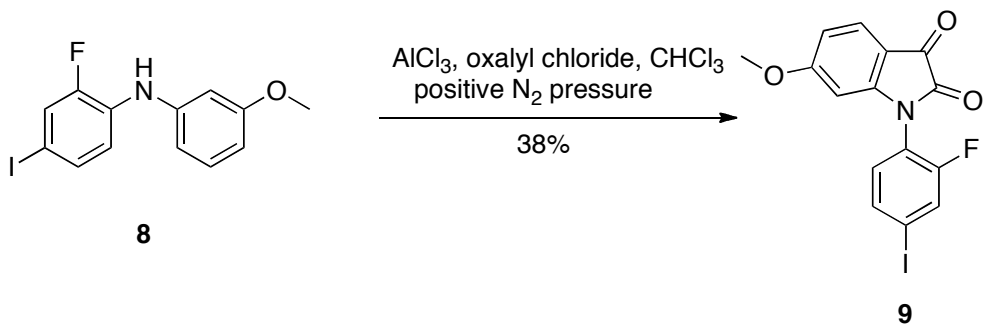

Figure 23: Formation of isatin **9**.

This reaction is water-sensitive, so it must be conducted with oven-dried glassware under positive nitrogen pressure. It is also essential to use amylene-stabilized chloroform because of the risk of the production of the ethyl ester if any ethanol has been used as a preservative in the solvent.[19,22] This reaction series is highly selective, due to the deactivated fluoro-iodo benzene ring and the electron donating methoxy group.

Diphenylamine **8** is added drop-wise to a solution of oxalyl chloride in amylene-stabilized chloroform. The lone pair on the nitrogen of diphenylamine **8** attacks one of the carbonyl carbons of oxalyl chloride to give an amide (Figure 24). At this point, the solvent and excess acetyl chloride are removed *in vacuo*, the product is redissolved in dichloromethane (DCM), and aluminum chloride is added. The aluminum complexes to the acid chloride, putting a positive charge on the

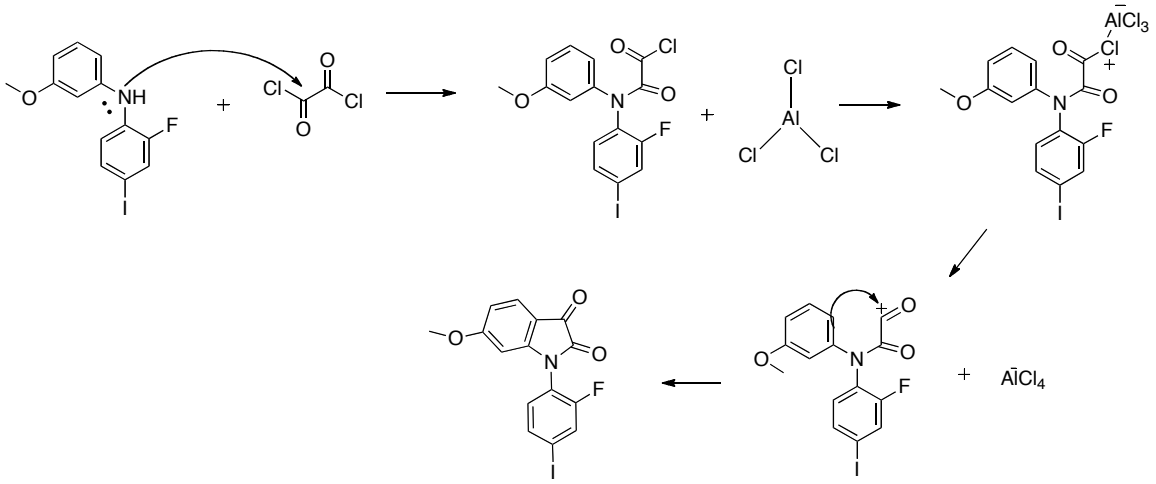

Figure 24: Ring-closing mechanism via Friedel-Crafts Acylation.

chloride and creating a good leaving group. The aluminum chloride complex leaves, creating a positively charged carbon. The pi electrons from the benzene ring donate into this carbon, closing the ring in a Friedel-Crafts Acylation.

Kieffer had converted isatin **9** into (*Z*)-1-(2-fluoro-4-iodophenyl)-3-(hydroxyimino)-6-methoxyindolin-2-one (**14**) through condensation with hydroxylamine hydrochloride (Figure 25).[19] This reaction proceeded in 44% yield and selective conversion of the ketone at position 1 was observed.[19] She then

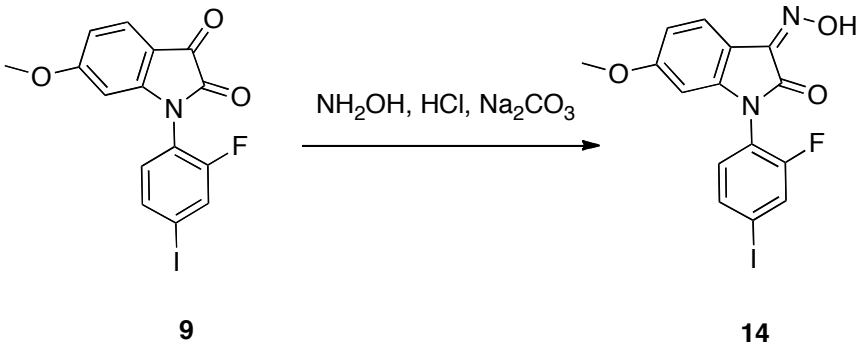

9 **14**

Figure 25: Formation of oxime **14**.[19]

attempted to convert oxime **14** into 3-amino-1-(2-fluoro-4-iodophenyl)-6-methoxyindolin-2-one (**10**) via a hydrogenation reaction based on the procedure of Carlo, et al. (Figure 26).[19,27] Hydrogenation with a palladium catalyst produced only trace amounts of the desired amine **10**, due to cleavage of the iodine, so other reaction conditions were tested.[19] However, NMR analysis showed little evidence of

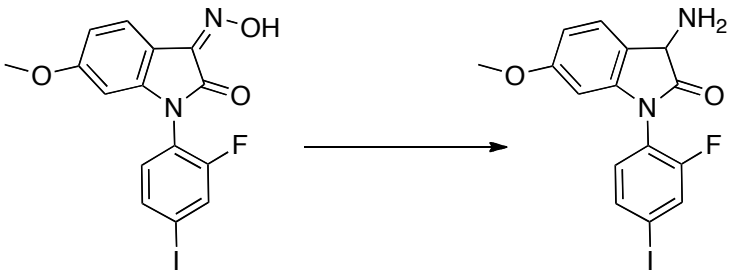

14 **10**

Figure 26: Attempted formation of amine **10** through various methods.[19]

the desired product with any method.

Kieffer's results prompted a need for an alternative method to produce amine **10**. We decided to pursue a method excluding the oxime intermediate, since hydrogenation seemed an impractical method for converting between oxime to amine. Therefore, we want to pursue an alternative method of reduction to form amine **10** from isatin **9**. Reductive amination has been shown to be a good method to produce such primary amines. Dangerfield, et al. created a methodology for a sans protecting group reductive amination to form primary amines.[28] They demonstrated that primary amines could be produced via metal hydride reductive amination with

close attention to a few reaction conditions, including the number of amine equivalents, the pH, and the concentration of ammonia. They found that by using activated Zn, $NaCNBH_3$, and 30% aqueous NH_3 in saturated NH_4OAc in EtOH, they could reduce a variety of substrates in a fast and efficient manner.[28] However, sodium cyanoborohydride ($NaCNBH_3$) produces toxic byproducts, making it an undesirable reagent. Furthermore, Dangerfield, et al. focused on the reductive amination of aldehydes, while we are interested in reducing ketones.

We continued to explore other methods for the reductive amination of ketones, and found that Ramachandran, et al. produced a variety of primary, secondary, and tertiary amines from ketones via reductive amination.[29] They saw excellent yields, but used an expensive reagent, ammonia borane. We wanted to avoid dangerous and expensive reagents, and instead found a practical procedure for the reductive amination of ketones and aldehydes using sodium triacetoxyborohydride ($NaBH(OAc)_3$) as the reducing agent and ammonium trifluoroacetate ($CF_3CO_2NH_4$) as the amine source.[30]

Based on the procedure of Carlson, et al., we developed reaction conditions for the reductive amination of isatin **9** (Figure 27).[30] Since this method had not yet

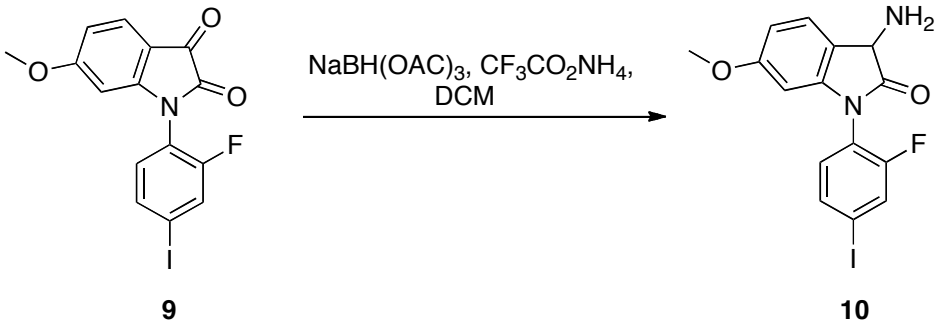

Figure 27: Proposed scheme for the formation of isatin **10**.

been tested on isatin **9** and it took 6 steps to produce isatin **9**, we decided to test the reaction on a model system (Figure 28). 1-(2-fluorophenyl)-6-methoxyindoline-2,3-dione (**15**) is easier and faster to produce than isatin **9**, and there are minimal

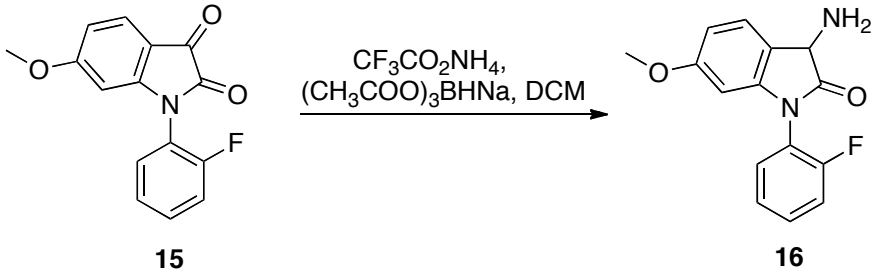

Figure 28: Formation of amine **16**.

changes to the overall structure, thus making it an ideal model compound.

Isatin **15** and $CF_3CO_2NH_4$ were added to a solution of DCM and stirred until dissolved. The $CF_3CO_2NH_4$ dissociates into $CF_3CO_2^-$ and NH_4^+. The ammonium acts as the nitrogen source, and the nitrogen attacks the carbonyl carbon in position one only (Figure 29). This attack is very selective because the carbonyl in position 1 is more electrophilic than the carbonyl in position 2. The carbonyl in position 2

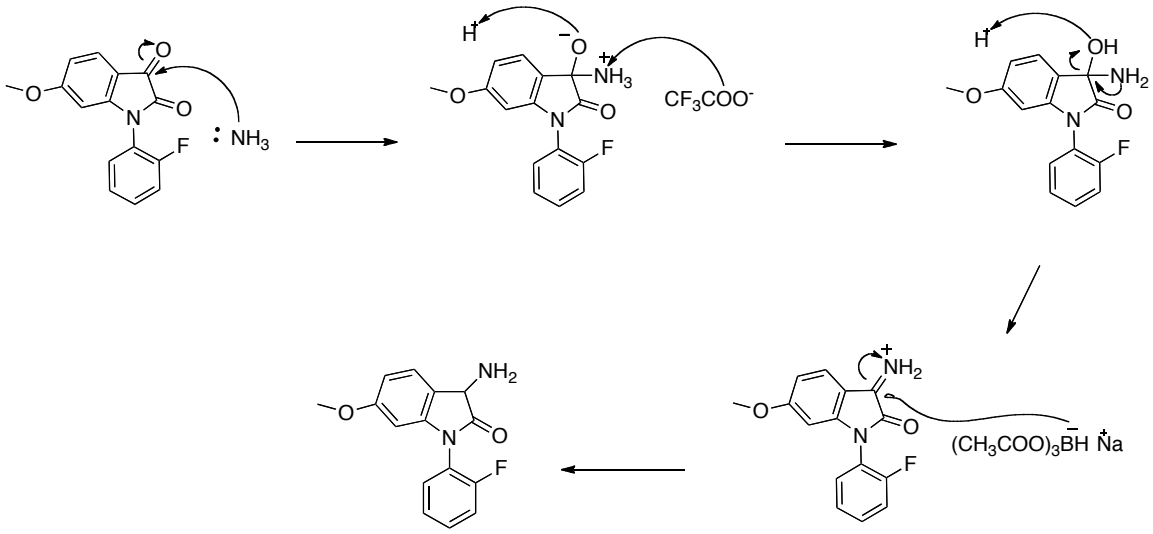

Figure 29: Mechanism of reductive amination to form amine **16**.

participates in an amide bond; the nitrogen bond increases the electron density on the carbon, thus decreasing its electrophilicity. Then, $NaBH(OAc)_3$ is then added to the solution, which is stirred at room temperature for 19 hours. The borohydride acts as the reducing agent, donating a hydride to the carbon in position one, creating a single bond between the carbon in position 1 and the nitrogen. The nitrogen is protonated as the reaction is quenched, thus forming the desired amine. After quenching, the product was impure, so column chromatography was used to purify the mixture. However, the amine product is susceptible to decomposition, which was observed during the purification process. In order to avoid excess decomposition, amine **16** must be converted into an HCl salt quickly.

Before attempting this reaction on isatin **9**, we wanted to optimize the reaction conditions to achieve a higher yield and to decrease or prevent decomposition. In order to do so, more of isatin **15** must be produced, so we

followed a 5 step synthetic scheme (Figure 30). The synthesis of **15** begins with *m*-anisidine (**3**), as did the synthesis of **1**. However, instead of coupling *m*-anisidine to

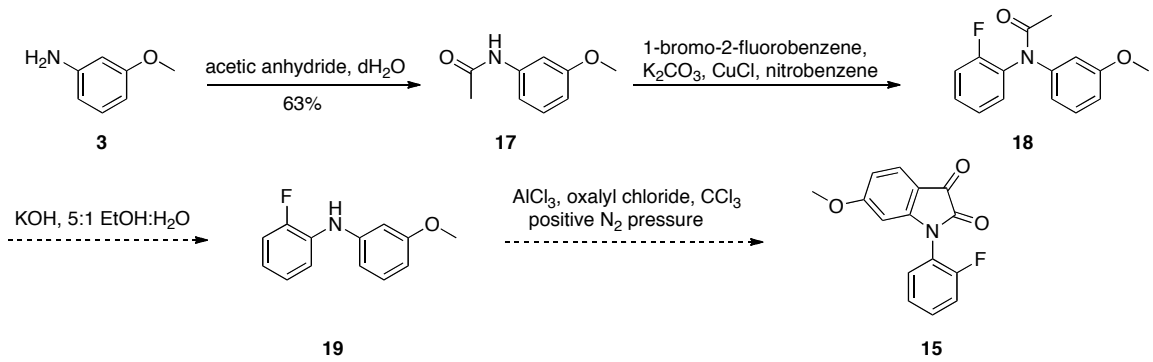

Figure 30: Formation of isatin **15** from *m*-anisidine (**3**).[22,31]

1-bromo-2-fluorobenzene first, we installed the acyl protecting group using acetic anhydride to produce N-(3-methoxyphenyl)acetamide (**17**) following the procedure designed by Anderson.[31]

Once the acyl group was installed, the coupling of acetamide **17** and 1-bromo-2-fluorobenzene was attempted, again following the procedure outlined by Anderson.[31] The reaction involved the use of potassium carbonate (K_2CO_3) and copper (I) chloride (CuCl) as a catalyst. The solution was stirred at 190° C for 24 hours. A color change was evident, indicating a reaction. However, no product was seen with GC-MS analysis. Since 1-bromo-2-fluorobenzene has a boiling point of 155° C, it could have boiled off before the reaction had time to proceed to completion. The second attempt at this reaction was conducted at 130° C for 23 hours. A black oil was produced, but there was still no evidence of the desired product, acetamide **18**. In the future, different conditions should be tested on this

reaction, including temperature and concentration of CuCl, in order to produce product and optimize the yield.

Conclusion

Significant progress toward the synthesis of azido T-0632 analog **1** has been made. A modification to the iodination of **6** has been completed to gain a greater yield. A method has been designed to form amine **10** from isatin **9** bypassing the oxime intermediate. Completion of the synthesis of isatin **15** must be achieved, and then the reductive amination of isatin **15** to amine **16** must be optimized. Once this reaction is optimized, it should be tested on isatin **9** so that the synthesis of analog **1** can be completed. By completing the synthetic pathway to produce compound **1**, we are preparing for biological and structural studies of the interaction between T-0632 and GLP-1R. The results of such studies will provide information on the structure of GLP-1R, and thus advance the search for alternative drug treatments for type II diabetes.

Experimental Methods

General

Commercial reagents were purchased from Sigma-Aldrich, Fischer, or Alfa-Aesar and used without further purification. Air and water sensitive reactions were conducted with oven-dried glassware fitted with a rubber septa under positive nitrogen pressure. Thin-layer chromatography was performed on Merck 60-F_{254} pre-coated silica gel plates, which were visualized by exposure to ultraviolet (UV) light at 254 nm. Column chromatography was performed using Sigma-Aldrich silica gel (60 Å, 70-230 mesh). Flash chromatography was performed using Biotage FLASH silica cartridges for the SP1 system. All NMR spectra were taken using a Bruker 300 MHz WIN-NMR spectrometer with TMS as an internal standard. Mass spectra were recorded with an Agilent 6890N Network GC System coupled with an electron impact Agilent 5837 Network Mass Selective Detector. The method used for GC-MS analysis is "RAYANNE" ($T_{initial}$=120°C, T_{final}=325°C, rate=20°C/sec; split mode (inlet); mobile phase=$He_{(g)}$; constant flow mode, flow rate=1.0 ml/min; injection volume=1.0µl; pressure=11.6 psi).

*Analog **1***

2-Fluoro-N-(3-methoxyphenyl)-4-nitroaniline (4)[19]

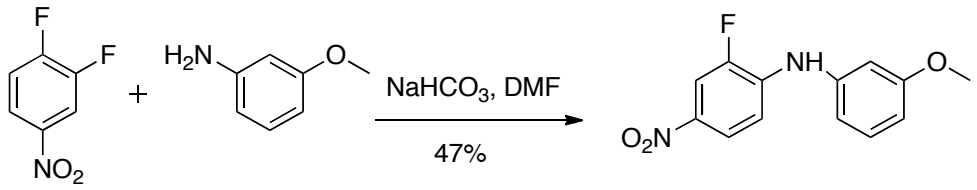

2 **3** **4**

To a solution of 1,2-difluoro-4-nitrobenzene (**2**) (10 g, 62.9 mmol) and m-anisidine (**3**) (10.5 mL, 94.3 mmol) dissolved in DMF (10 mL), sodium bicarbonate (5.3 g, 62.9 mmol) was added. The solution was then stirred at 80° C for 6 days. The reaction mixture was quenched with 10% HCl and subsequently extracted with DCM. The organic layers were washed with brine, dried over magnesium sulfate, and filtered, resulting in a brownish-red solution. The solvent was removed *in vacuo*. Passage through a silica plug (1:1 EtOAc: Hex) and recrystallization from hot EtOH/dH_2O yielded orange crystals (7.8 g, 47%). GC-MS: M+,m/z=262. ^{1}H-NMR ($CDCl_3$, 300 MHz): δ 8.0 (m, 2H), 7.25 (m, 3H), 6.75 (m, 2H), 6.3 (s, 1H), 3.8 (s, 3H).

N-(2-Fluoro-4-nitrophenyl)-N-(3-methoxyphenyl)acetamide (5)[19]

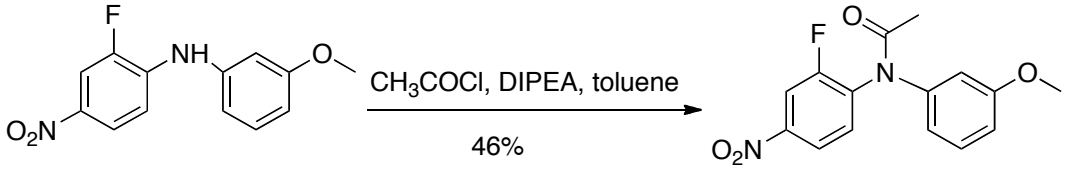

4 **5**

Toluene (150 mL) was added to a roundbottom flask containing diphenylamine **4** (5.22g, 19.9 mmol), and the solution was boiled for 20 minutes to remove residual

water. The flask was then placed under positive nitrogen pressure and acetyl chloride (8.46 mL, 119.9 mmol) was added dropwise, resulting in a rust-colored solution. Diisopropylethylamine (13.8 mL, 79.6 mmol) was then added dropwise, resulting in the evolution of white vapors. After the vapors dissipated, the solution is a cloudy, red-orange color with a white precipitate. The solution was stirred at room temperature overnight. After 12 hours, the solution was quenched with 5% HCl and extracted with DCM. The organic layers were washed with brine, dried over magnesium sulfate, and filtered. Column chromatography (silica gel, 10-25% EtOAc in Hexanes) and removal of the solvent *in vacuo* yielded a viscous, yellow oil (2.4g, 46%). GC-MS: M+,m/z=304. ^{1}H-NMR ($CDCl_3$, 300 MHz): δ 8.1 (m, 2H), 7.4 (m, 3H), 6.9 (m, 2H), 4.2 (m, impurity), 3.85 (s, 3H), 2.2 (s, 3H).

N-(4-Amino-2-fluorophenyl)-N-(3-methoxyphenyl)acetamide (6)[19,23]

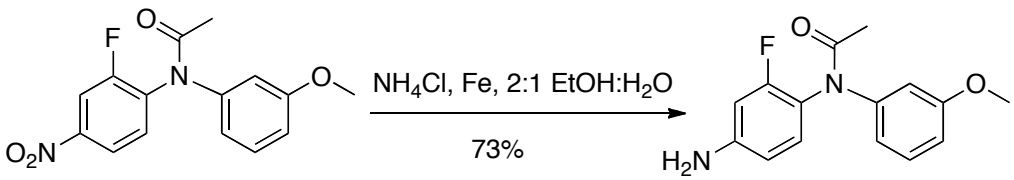

5 **6**

Acetamide **5** (0.38 g, 1.2 mmol) and ammonium chloride (0.63 g, 11.8 mmol) were dissolved in a solution of 2:1 EtOH:dH_2O (12 mL), and the solution was brought to reflux. Iron powder (0.20 g, 2.5 mmol) was added over the course of 30 minutes. The solution was stirred at reflux for an hour and then stirred at room temperature for an additional 3 hours. The solution was filtered through celite, and the ethanol was removed *in vacuo*. The organic layer was extracted with DCM, washed with

brine, dried over magnesium sulfate, and filtered. The solvent was removed *in vacuo*, yielding a viscous, red-brown oil (0.24 g, 73%). No further purification was necessary. GC-MS: M+,m/z=274.

N-(2-Fluoro-4-iodophenyl)-N-(3-methoxyphenyl)acetamide (7)[19,24]

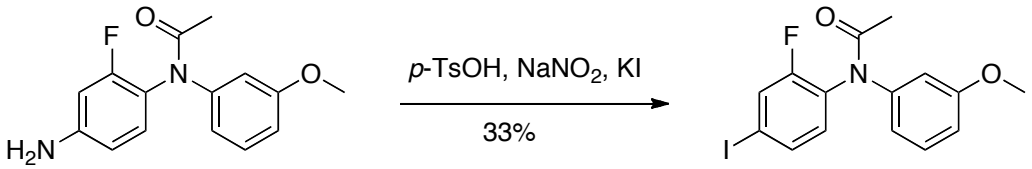

6 **7**

Attempt 1: Amine **6** (0.20 g, 0.73 mmol) was dissolved in DCM and added to a mortar containing p-TsOH (0.42 g, 2.21 mmol). The DCM was allowed to evaporate. The amine and p-TsOH were ground with the pestle for five minutes, upon which time $NaNO_2$ (0.13 g, 1.88 mmol) was added. The resulting paste immediately became a deep red color and was ground for ten minutes. Then, KI (0.12 g, 0.72 mmol) was added and the paste became much more viscous and turned a dark brown color. After grinding intermittently for 20 minutes, the reaction was quenched with 10% Na_2SO_3 (15 mL), turning the solution a mustard yellow. The solution was allowed to sit for an hour, and a brown precipitate was evident. The product was washed into a separatory funnel containing brine, DCM, and diethyl ether. The organic layer was collected, washed with brine, dried over $MgSO_4$, and filtered. Column chromatography (silica gel, 30-40% EtOAc in Hexanes) and removal of the solvent *in vacuo* yielded a red oil (0.09 g, 32%).

Attempt 2: Amine **6** (0.19 g, 0.69 mmol) was dissolved in DCM and added to a mortar containing silica gel (0.40 g). Upon evaporation of the DCM, p-TsOH (0.40 g, 2.1 mmol) was added to the mortar. The amine and p-TsOH were ground with the pestle for five minutes, upon which time $NaNO_2$ (0.12 g, 1.7 mmol) was added. The resulting paste immediately became a cherry red color and was ground for ten minutes. Then, KI (0.12 g, 0.72 mmol) was added and the paste became a red-brown powder. After grinding intermittently for 20 minutes, the reaction was quenched with 10% Na_2SO_3 (15 mL), turning the solution a bright orange. The solution was allowed to sit for an hour, and an orange precipitate was evident. The product was washed into a separatory funnel containing brine, DCM, and diethyl ether. The organic layer was collected, washed with brine, dried over $MgSO_4$, and filtered. No product was formed.

Attempt 3: Amine **6** (0.21 g, 0.76 mmol) was dissolved in DCM and added to a mortar containing p-TsOH (0.42 g, 2.21 mmol). The DCM was allowed to evaporate, and the mortar was placed on ice. The amine and p-TsOH were ground with the pestle for five minutes, upon which time $NaNO_2$ (0.13 g, 1.88 mmol) was added. The resulting paste immediately became a cherry red color and was ground for ten minutes. Then, KI (0.13 g, 0.78 mmol) was added and the paste became much more viscous and turned an orange-brown color. The mortar was removed from ice. After grinding intermittently for 20 minutes, the reaction was quenched with 10% Na_2SO_3 (15 mL), turning the solution a bright orange. The solution was allowed to sit for an hour, and a brown precipitate was evident. The product was washed into a

separatory funnel containing brine, DCM, and diethyl ether. The organic layer was collected, washed with brine, dried over $MgSO_4$, and filtered. Column chromatography (silica gel, 30-40% EtOAc in Hexanes) and removal of the solvent *in vacuo* yielded a red oil (0.05 g, 17%).

Attempt 4: Amine **6** (0.24 g, 0.88 mmol) was dissolved in DCM and added to a mortar containing p-TsOH (0.50 g, 2.6 mmol). The DCM was allowed to evaporate and the solution was placed on ice. The amine and p-TsOH were ground with the pestle for five minutes, upon which time $NaNO_2$ (0.15 g, 2.2 mmol) was added. The resulting paste immediately became a bright red color and was ground for ten minutes. Then, KI (0.36 g, 2.2 mmol) was added and the mortar was removed from the ice bath; the paste became much more viscous and turned an orange-brown color. After grinding intermittently for 20 minutes, the reaction was quenched with 10% Na_2SO_3 (15 mL), turning the solution a bright orange. The solution was allowed to sit for an hour, and 2 layers became evident: a red precipitate and an orange liquid. The product was washed into a separatory funnel containing brine with DCM. The organic layer was collected, washed with brine, dried over $MgSO_4$, and filtered. Column chromatography (silica gel, 30-40% EtOAc in Hexanes) and removal of the solvent *in vacuo* yielded a red oil (0.12 g, 33%). GC-MS: M+, m/z=385. ^{1}H-NMR ($CDCl_3$, 300 MHz): δ 7.5-6.7 (m, 7H), 5.3-5.0 (m, impurity), 3.75 (s, 3H), 3.7 (m, impurity), 2.1 (s, 3H), 1.4-1.1 (m, impurity).

2-Fluoro-4-iodo-N-(3-methoxyphenyl)aniline (8)[19,25,26]

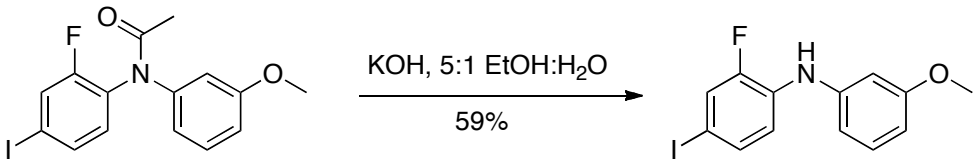

7 **8**

Acetamide **7** (100.3 mg, 0.26 mmol) and potassium hydroxide (43.9 mg, 0.78 mmol) were dissolved in a solution of 5:1 EtOH:dH_2O (6 mL). The solution was stirred at 60° C for 6 hours. The solution was cooled to room temperature, and the organic layer was extracted with DCM, washed with brine, dried over $MgSO_4$, and then filtered. The solvent was removed *in vacuo*, yielding a viscous, red-brown oil (53 mg, 59%). No further purification was necessary. GC-MS: M+, m/z=343. ^{1}H-NMR ($CDCl_3$, 300 MHz): δ 7.5-7.1 (m, 4H), 6.7 (m, 2H), 6.8 (s, IH), 3.85 (s, 3H).

1-(2-fluoro-4-iodophenyl)-6-methoxyindoline-2,3-dione (9)[19,22,32,33]

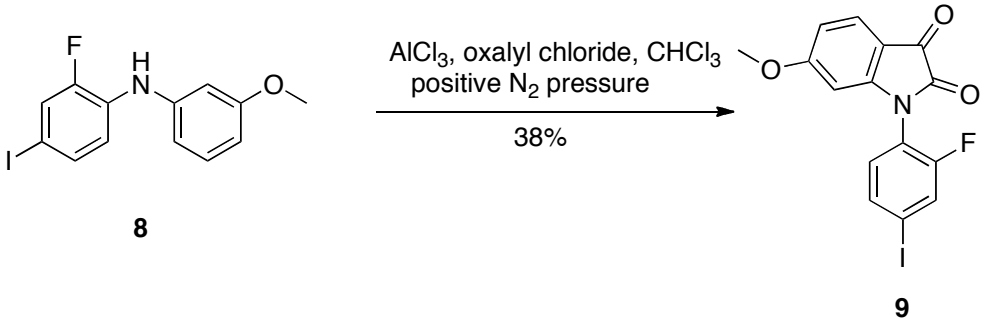

8 **9**

Oxalyl chloride (55μL, 0.647 mmol) was dissolved in amylene-stabilized chloroform (1mL) in a flame-dried roundbottom flask, which was placed under positive nitrogen pressure. The flask was placed in an ice bath, and diphenylamine **8** (55.5mg, 0.162mmol)**,** which was dissolved in amylene-stabilized chloroform

(1mL), was added dropwise. The reaction mixture was stirred at room temperature for 2.5 hours. The purple solution was concentrated *in vacuo* and redissolved in amylene-stabilized chloroform. This process was repeated twice. The resulting purple solid was dissolved in DCM (2mL), and the solution was cooled to 0°C. To this solution, $AlCl_3$ (22 mg, 0.162mmol) was added. The solution was allowed to reach room temperature, and the flask was flushed with N_2 and sealed. The solution was stirred at room temperature for 4 days. The solution was diluted with DCM and poured into ice and concentrated HCl. Once the ice had melted, the organic layer was extracted with DCM three times, washed with brine, dried over sodium sulfate, and filtered. Column chromatography (silica gel, 10-30% EtOAc in Hexanes) and removal of the solvent *in vacuo* yielded an orange solid (0.024g, 38%). GC-MS: M+, m/z=397. ^{1}H-NMR ($CDCl_3$, 300 MHz): δ 7.85 (d, 1H), 7.3 (s, 1H), 7.2 (t, 2H), 6.7 (d, 1H), 6.2 (s, 1H), 3.9 (s, 3H), 1.7 (s, impurity).

3-Amino-1-(2-fluorophenyl)-6-methoxyindolin-2-one (16)[30]

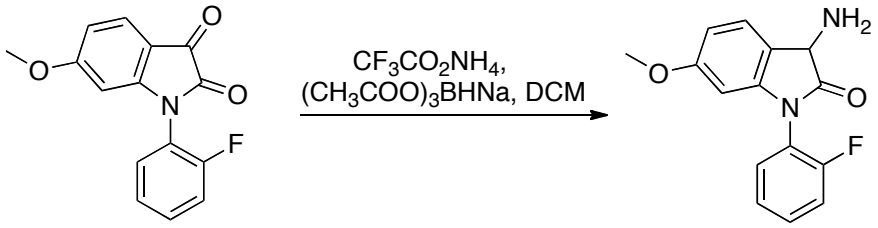

15 **16**

To a solution of DCM (100mL) was added isatin **15** (0.96 g, 3.56mmol) and ammonium trifluoroacetate (0.69g, 5.33mmol). Once a solution was achieved, the sodium triacetoxyborohyride (1.13g, 5.33mmol) was added, and the resulting solution was stirred at room temperature for 19 hours. The reaction mixture was

quenched with 5% $NAHCO_3$ and the organic layer was extracted with water 3 times, dried over sodium sulfate, and filtered. Column chromatography (silica gel, 0.4% MeOH in DCM) and the removal of solvent *in vacuo* yielded a green solid. The solid was dissolved in EtOH, and HCl (1 ml) was added. The solvent and excess HCl were removed *in vacuo*. The solid was dissolved in ether (30 mL), and the solvent was removed *in vacuo*, yielding a brown-yellow solid. GC-MS: M+, m/z=273. ^{1}H-NMR ($CDCl_3$, 300 MHz): δ 7.8 (s, 1H), 7.3 (m, 6H), 5.2 (m, 2H), 3.75-3.4 (m, 1H), 1.5 (s, 3H).

N-(3-Methoxyphenyl)acetamide (17)[31]

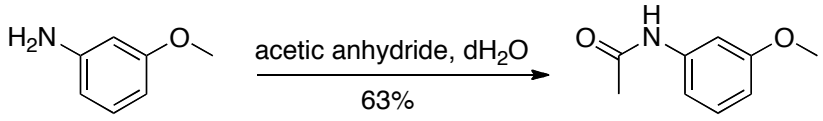

3 **17**

A solution of **3** (2.5mL, 22.3mmol) and dH_2O (20mL) was stirred for 5 minutes. To this solution, acetic anhydride (4.25mL, 44.7mmol) was added dropwise. The solution was stirred at room temperature for 2 hours. Then, the solution was cooled to 0°C, and a tan solid precipitated. Vacuum filtration yielded impure solid. Recrystallization in 1:1 dH_2O:EtOH yielded tan crystals (2.3g, 63%). GC-MS: M+, m/z=165. ^{1}H-NMR ($CDCl_3$, 300 MHz): δ 7.3 (m, 1H), 7.0 (d, 2H), 6.7 (d, 1H), 3.8 (s, 1H), 2.25 (s, 3H), 1.65 (s, 3H).

***N*-(2-Fluorophenyl)-*N*-(3-methoxyphenyl)acetamide (16)**[31]

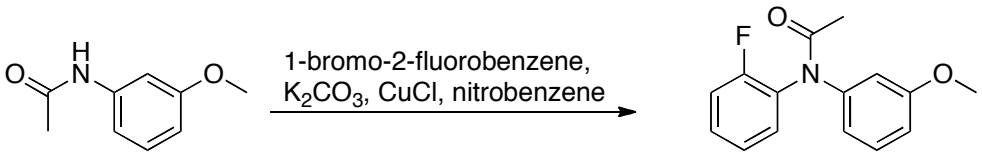

17 **18**

Attempt 1: To a solution of acetamide **17** (0.95g, 5.79mmol) and nitrobenzene (16 ml) was added 1-bromo-2-fluorobenzene (1.26ml, 11.6mmol), K_2CO_3 (0.88g, 6.37mmol), and CuCl (0.23g, 2.32mmol). The solution was heated to 190°C and stirred for 24 hours. The solution was cooled to room temperature and filtered through a silica plug with DCM. No product was formed.

Attempt 2: To a solution of acetamide **17** (0.98g, 5.97mmol) and nitrobenzene (20 ml) was added 1-bromo-2-fluorobenzene (1.31ml, 11.95mmol), K_2CO_3 (0.91g, 6.57mmol), and CuCl (0.24g, 2.4mmol). The solution was heated to 130°C and stirred for 23 hours. The solution was cooled to room temperature and vacuum filtered through a celite plug with DCM. No product was formed.

References

1. Diabetes Statistics. Retrieved from www.diabetes.org/diabetes-basics/diabetes-statistics/. (July 16, 2010).
2. Type 2 Diabetes. Retrieved from www.mayoclinic.com/health/type-2-diabetes/DS00585. (July 16, 2010).
3. Maedler, K; Donath, M.Y. *Horm. Res.* **2004**; 62 Suppl3: 67-73.
4. Vilsbøll, T., Knop, F.K. *BioDrugs*, **2008**, 22(4): 251-257.
5. Perfetti, R., Merkel, P. *Eur. J. Endocrinol.* **2000**, *143*, 717-725.
6. Bowen, R. *Physiological Effects of Insulin* 2009 [cited January 9, 2012. Available from http://www.vivo.colostate.edu/hbooks/pathphys/endocrine/pancreas/insulin_phys.html.
7. Chia, C.W; Egan, J.M. *Diabetes, Metabolic Syndrome and Obesity: Targets and Therapy*, **2009**, 2, 37-49.
8. Runge, S., Thøgersen, H., Madsen, K., Lau, J., Rudolph, R. *J. Biol. Chem.* **2008**, *283*, 11340-11347.
9. Xiao, Q., Jeng, J., Wheeler, M.B. *J. Mol. Endocrinol.* **2000**, *25*, 321-335.
10. Adelhorst, K., Hedegaard, B.B., Knudsen, L.B., Kirk, O. *J. Biol. Chem.* **1994**, *269*, 6275-6278.
11. Donnelly, D. *FEBS Letters* **1997**, *409*, 431-436.
12. Dong, M., Gao, F., Pinon, D.I., Miller, L.J. *Mol. Endocrinol.* **2008**, *22*, 1489-1499.
13. Chen, Q. M., L.J., Dong, M. *Am. J. Physiol. Endocrinol. Metab.* **2010**, *299*, E62-E68.

14. Miller, L. J., Chen, Q., Lam, P.C.-H., Pinon, D.I., Sexton, P.M., Abagyan, R., Dong, M. *J. Biol. Chem.* **2011**, *286*, 15895-15907.
15. Arulmozhi, D. K.; Portha, B. *European Journal of Pharmaceutical Sciences,* **2006**, 28(1-2), 96-108.
16. Shyangdan, D.S., Royle, P.L., Sharma, P., Waugh, N.R. *BMC Endocr Disord*, **2010**, 20.
17. Addison, D., Aguilar, D. *Curr Atheroscler Rep*. **2011**, 13, 115-122.
18. Tibaduiza, E. C., Chen, C., Beinborn, M. *J. Biol. Chem.* **2001**, *276*, 37787-37793.
19. Kieffer, M. E., *Structural Studies of the Glucagon-like Peptide-1 receptor using photolabile analogs of a selective inhibitor*. Haines Research Group, Wellesley College, **2010**.
20. Chen, Q., Pinon, D.I., Miller, L.J., Dong, M. *J. Biol. Chem.* **2009**, *284*, 34135-34144.
21. Eberle, A. N., Graan, P.N.E.D *Methods in Enzymol.* **1985**, *109*, 129-156.
22. Kim, L., *The synthesis of the Glucagon-like peptide-1 receptor antagonist, T-0632*. Haines Research Group, Wellesley College, **2008**.
23. Renslo, A. R., Jaishankar, R., Venkatachalam, R., Hackbarth, C., Lopez, S., Patel, D.V., Gordeev, M.F. *J. Med. Chem* **2005**, *48*, 5009-5024.
24. Gorlushko, D. A., Filimonov, V.D., Krasnokutskaya, E.A., Semenischeva, N.I., Go, B.S., Hwang, H.Y., Cha, E.H., Chi, K.-W. *Tetrahedron Letters* **2008**, *49*, 1080-1082.
25. Kieth, D. D., Yang, R., Tortora, J.A., Weigele, M. *J. Org. Chem* **1978**, *43*, 3713-3716.

26. Dilbeck, G. A., Field, L., Gallo, A.A., Gargiulo, R.J. *J. Org. Chem.* **1978**, *43*, 4593-4596.

27. Carlo, F. J. D., Lindwall, H.G. *J. Am. Chem. Soc* **1945**, *67*, 199-201.

28. Dangerfield, E. M., Plunkett, C.H., Win-Mason, A.L., Stocker, B.L., Timmer, M.S.M. *J. Org. Chem* **2010**, *75*, 5470-5477.

29. Ramachandran, P. V., Gagare, P.D., Sakavuyi, K., Clark, P. *Tetrahedron Letters* **2010**, *51*, 3167-3169.

30. Carlson, M. W., Ciszewski, J.T., Bhatti, M.M., Swanson, W.F., Wilson, A.M. *J. Chem. Ed.* **2000**, *77*, 270-271.

31. Shelby Anderson. Laboratory Notebook, Wellesley College, Summer 2011.

32. Moser, P., Sallmann, A., Wiesenberg, I. *J. Med. Chem* **1990**, *33*, 2358-2368

33. Ben-Ishal, D., Sataty, I., Peled, N., Goldshare, R. *Tetrahedron* **1987**, *43*, 439-450.

Index of Appendices

Appendix

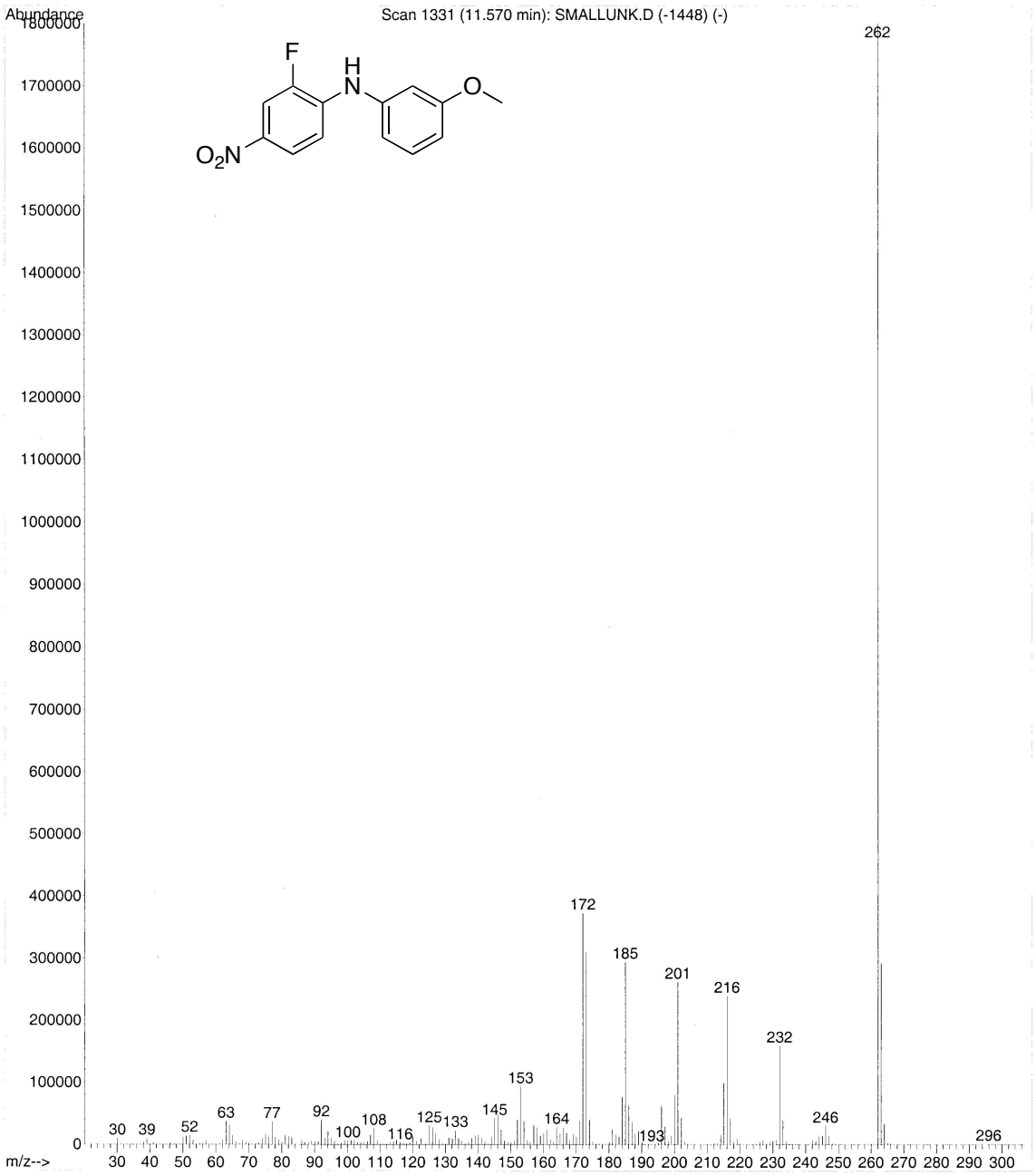
Abundance
Scan 1331 (11.570 min): SMALLUNK.D (-1448) (-)
F
H
N
O
O_2N
1800000
1700000
1600000
1500000
1400000
1300000
1200000
1100000
1000000
900000
800000
700000
600000
500000
400000
300000
200000
100000
0
m/z-->
30 40 50 60 70 80 90 100 110 120 130 140 150 160 170 180 190 200 210 220 230 240 250 260 270 280 290 300
262
172
185
201
216
232
153
246
296
63
77
92
108
125
133
145
164
193
30
39
52
100
116

H-NMR of diphenyl amine

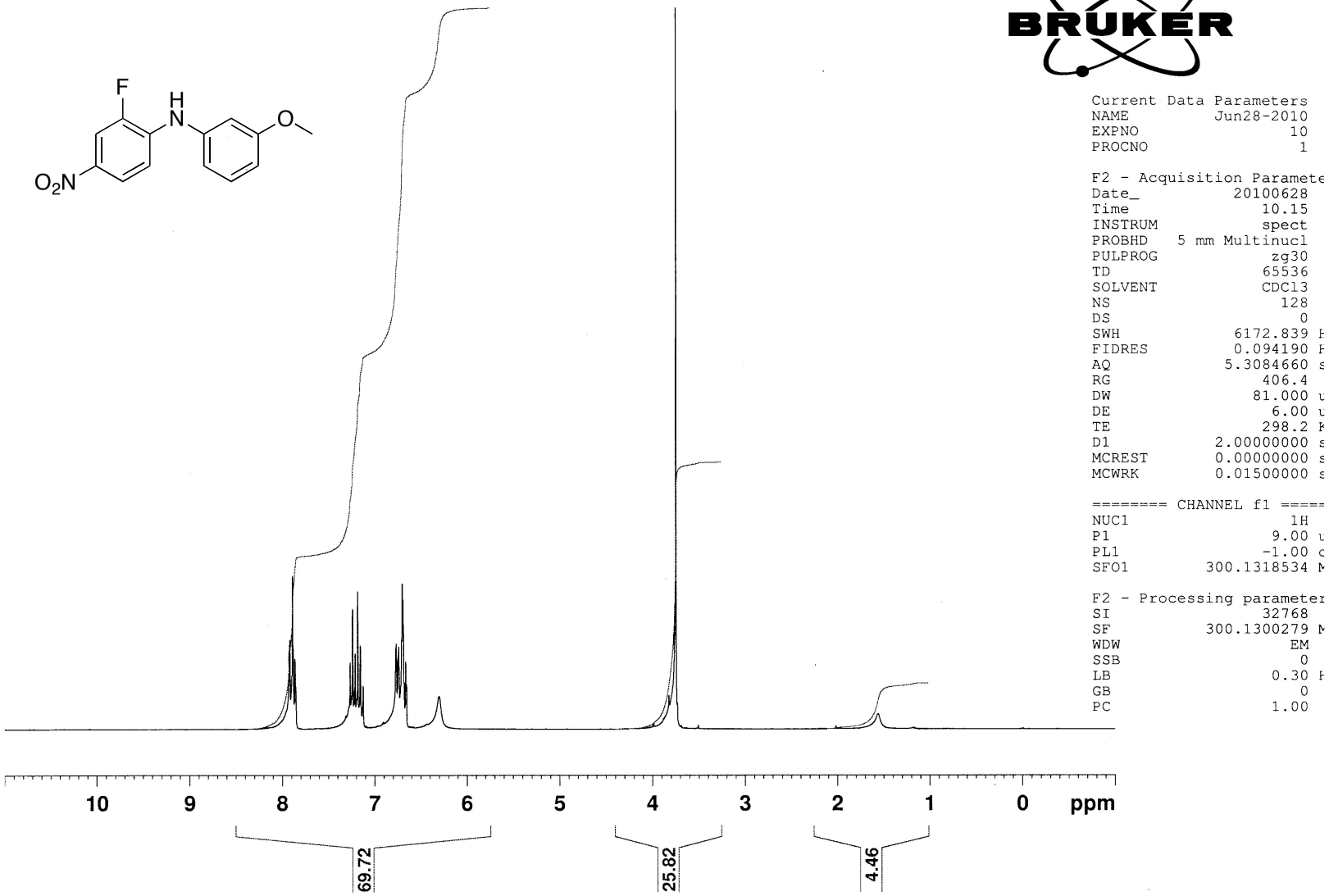

BRUKER

```
Current Data Parameters
NAME          Jun28-2010
EXPNO                 10
PROCNO                 1

F2 - Acquisition Parameter
Date_           20100628
Time               10.15
INSTRUM            spect
PROBHD   5 mm Multinucl
PULPROG             zg30
TD                 65536
SOLVENT            CDCl3
NS                   128
DS                     0
SWH             6172.839 H
FIDRES          0.094190 H
AQ              5.3084660 s
RG                 406.4
DW                81.000 u
DE                 6.00 u
TE                298.2 K
D1           2.00000000 s
MCREST       0.00000000 s
MCWRK        0.01500000 s

======== CHANNEL f1 =====
NUC1                  1H
P1                 9.00 u
PL1               -1.00 d
SFO1        300.1318534 M

F2 - Processing parameter
SI                 32768
SF          300.1300279 M
WDW                   EM
SSB                    0
LB                0.30 H
GB                     0
PC                 1.00
```

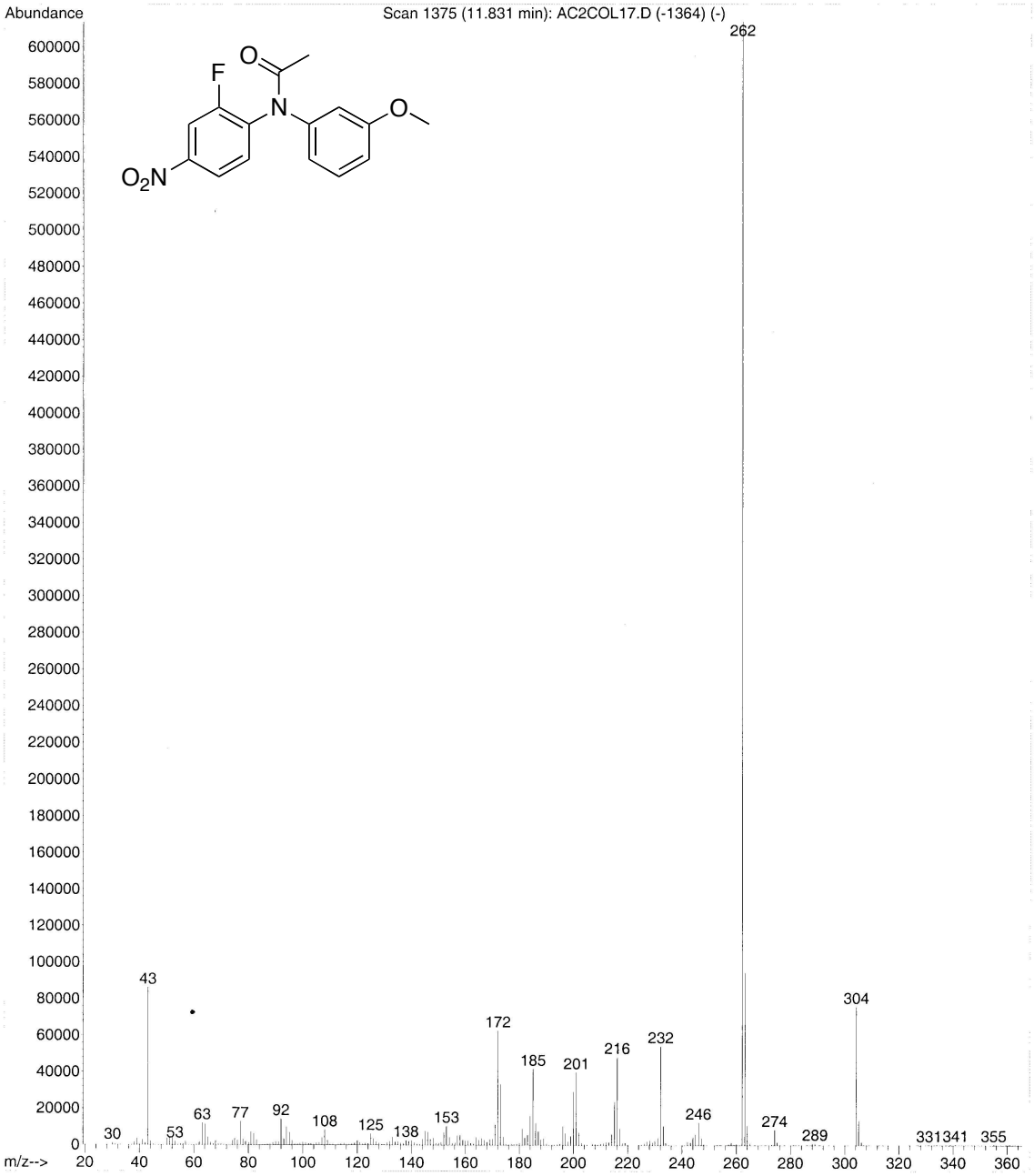
Abundance
Scan 1375 (11.831 min): AC2COL17.D (-1364) (-)
m/z-->
O
F
N
O
O2N
262
43
304
172
185
201
216
232
246
274
289
331341
355
63
77
92
108
125
138
153
30
53

H-NMR of acytelated DPA

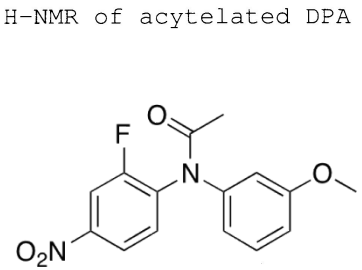


```
Current Data Parameters
NAME          Jul02-2010
EXPNO                 20
PROCNO                 1

F2 - Acquisition Paramete
Date_           20100702
Time               12.45
INSTRUM            spect
PROBHD   5 mm Multinucl
PULPROG             zg30
TD                 65536
SOLVENT            CDCl3
NS                   128
DS                     0
SWH             6172.839 H
FIDRES          0.094190 H
AQ              5.3084660 s
RG                   362
DW                81.000 u
DE                 6.00 u
TE                298.2 K
D1           2.00000000 s
MCREST       0.00000000 s
MCWRK        0.01500000 s

======== CHANNEL f1 =====
NUC1                 1H
P1                9.00 u
PL1              -1.00 d
SFO1        300.1318534 M

F2 - Processing parameter
SI                 32768
SF          300.1300000 M
WDW                   EM
SSB                    0
LB                0.30 H
GB                     0
PC                1.00
```

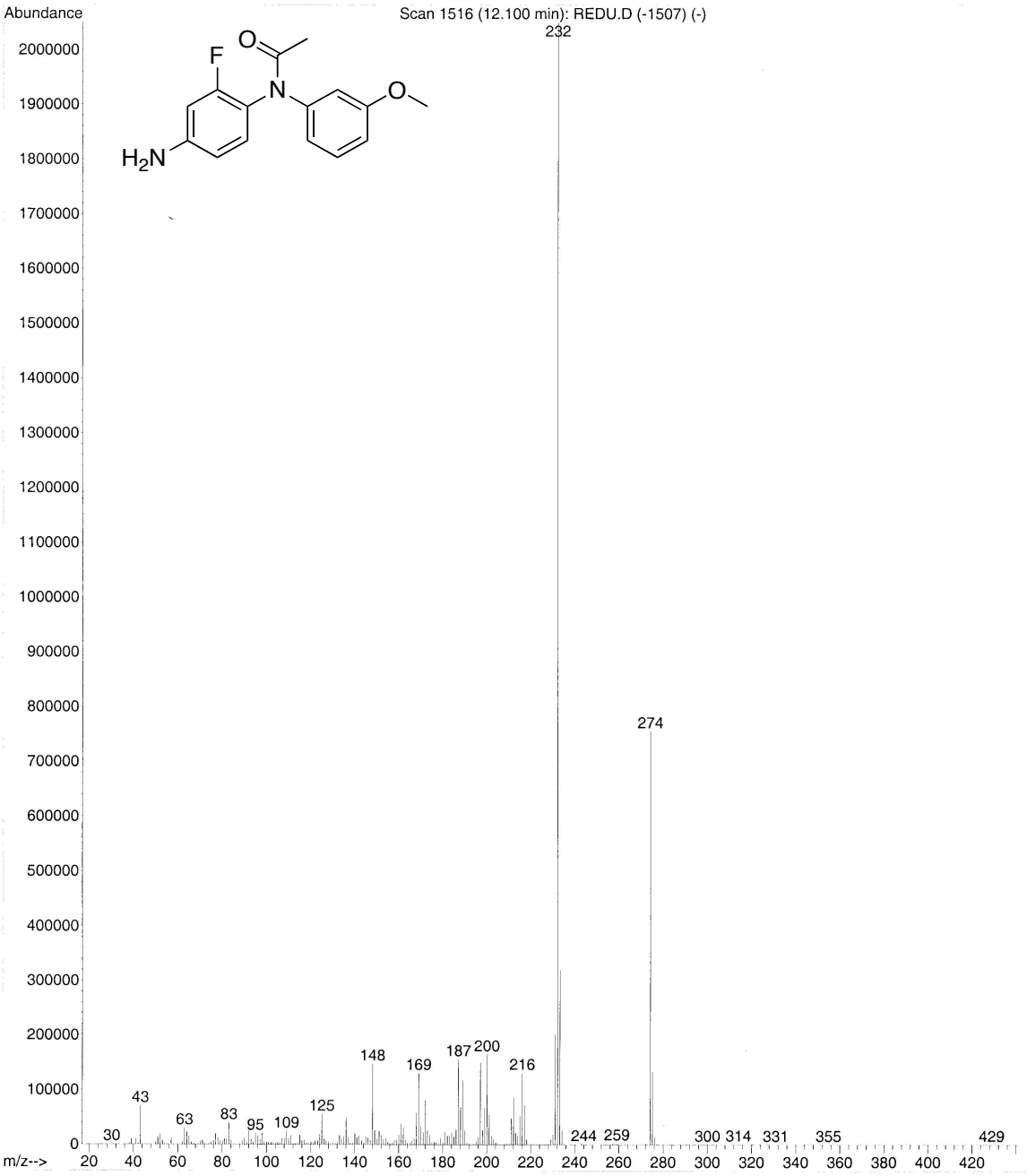
Abundance
Scan 1516 (12.100 min): REDU.D (-1507) (-)
232
274
148
169
187
200
216
125
43
63
83
95
109
30
244
259
300
314
331
355
429
m/z-->
F
O
N
O
H_2N

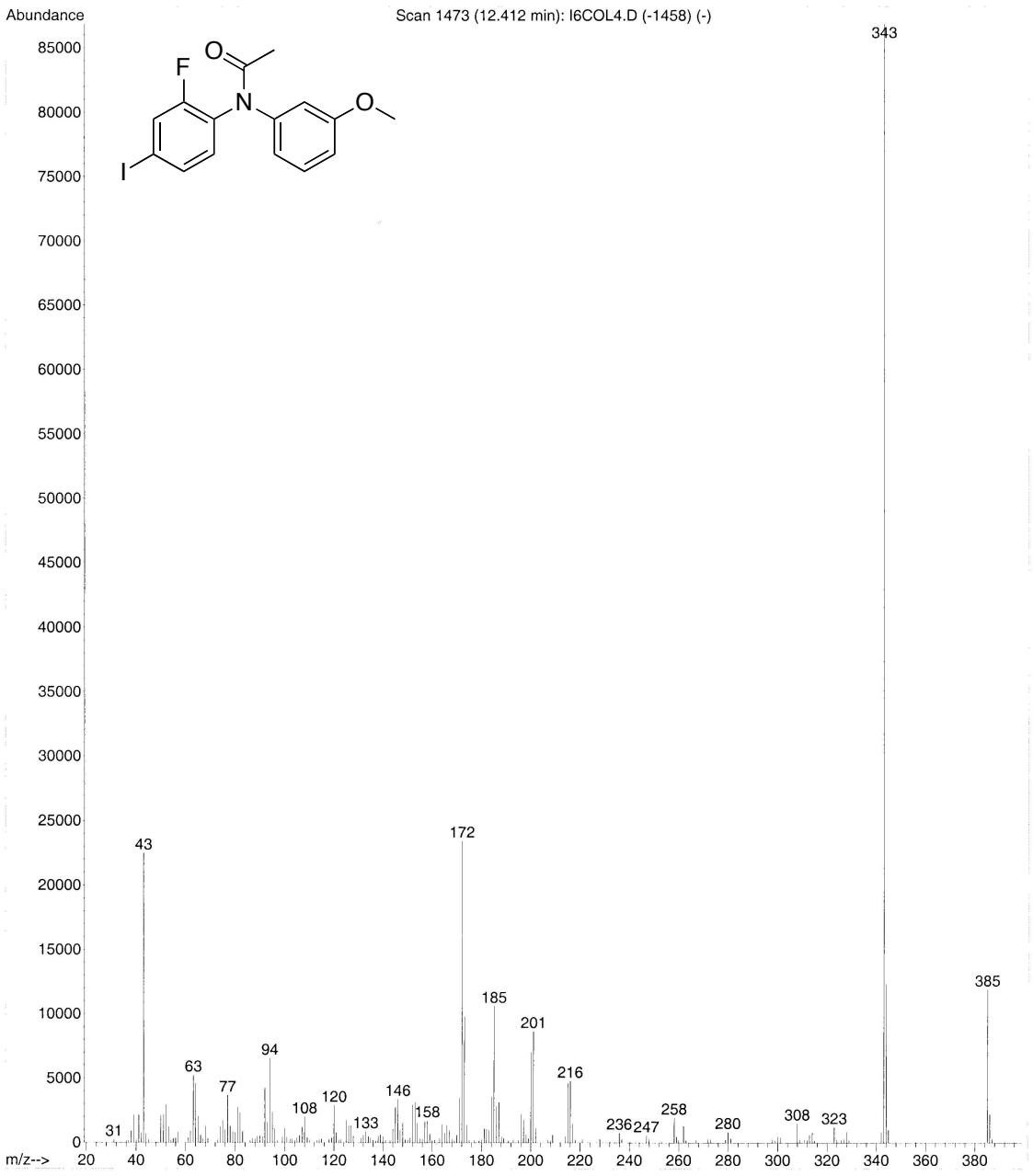
Abundance
Scan 1473 (12.412 min): I6COL4.D (-1458) (-)
85000
80000
75000
70000
65000
60000
55000
50000
45000
40000
35000
30000
25000
20000
15000
10000
5000
0
m/z-->
20 40 60 80 100 120 140 160 180 200 220 240 260 280 300 320 340 360 380
343
385
172
43
185
201
216
94
63
77
108
120
146
158
133
31
236
247
258
280
308
323
F
O
N
O
I

H-NMR of iodinated product

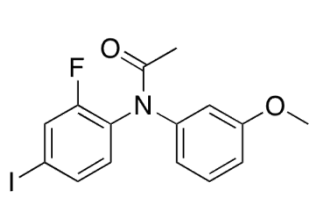

BRUKER

Current Data Parameters
NAME Jul08-2010
EXPNO 31
PROCNO 1

F2 - Acquisition Paramete
Date_ 20100709
Time 9.23
INSTRUM spect
PROBHD 5 mm Multinucl
PULPROG zg30
TD 65536
SOLVENT CDCl3
NS 128
DS 0
SWH 6172.839 H
FIDRES 0.094190 H
AQ 5.3084660 s
RG 256
DW 81.000 u
DE 6.00 u
TE 298.2 K
D1 2.00000000 s
MCREST 0.00000000 s
MCWRK 0.01500000 s

======== CHANNEL f1 =====
NUC1 1H
P1 9.00 u
PL1 -1.00 d
SFO1 300.1318534 M

F2 - Processing parameter
SI 32768
SF 300.1300263 M
WDW EM
SSB 0
LB 0.30 H
GB 0
PC 1.00

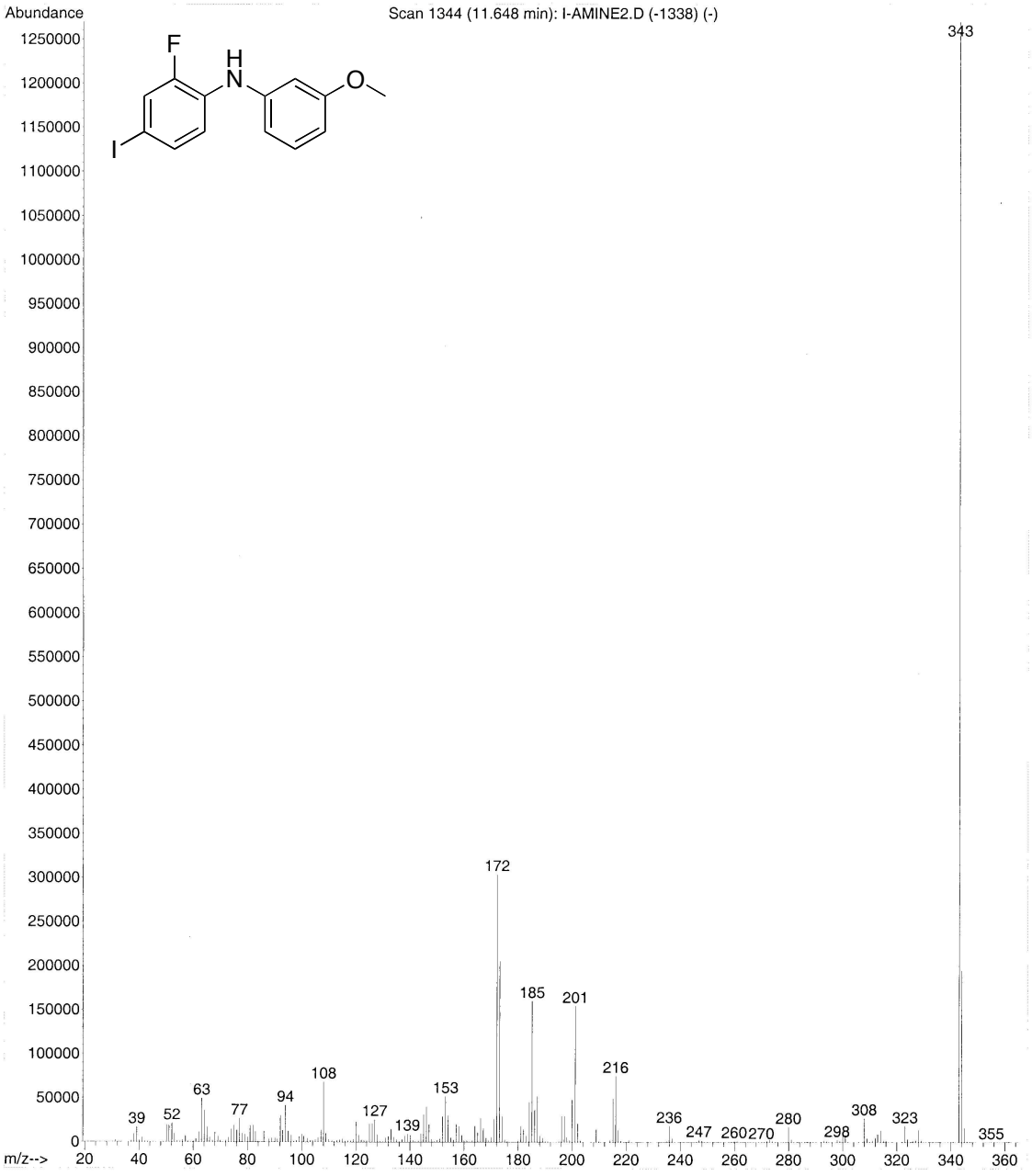
Abundance
Scan 1344 (11.648 min): I-AMINE2.D (-1338) (-)
F
H
N
O
I
343
172
185
201
216
108
63
94
153
77
127
139
39
52
236
247
260
270
280
298
308
323
355
m/z-->

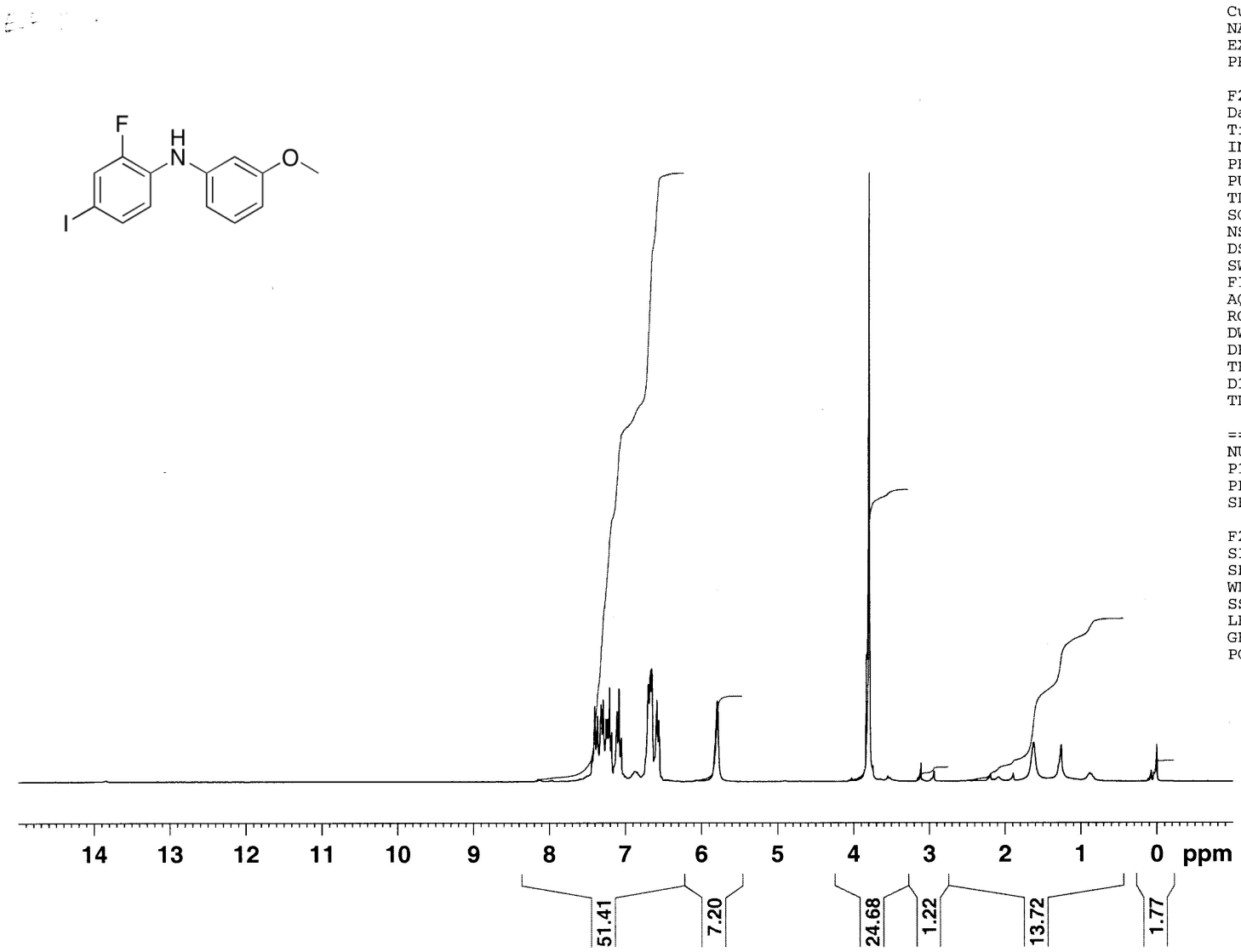


```
Current Data Parameters
NAME      Sep20-2011-dhai
EXPNO                  10
PROCNO                  1

F2 - Acquisition Paramet
Date_           20110920
Time               15.28
INSTRUM            spect
PROBHD   5 mm BBO BB-1H
PULPROG              zg
TD                32768
SOLVENT           CDCl3
NS                   16
DS                    0
SWH            5995.204
FIDRES         0.182959
AQ             2.7329011
RG                161.3
DW                83.400
DE                  6.00
TE                295.2
D1            2.00000000
TD0                   1

======== CHANNEL f1 ====
NUC1                 1H
P1                 9.00
PL1               -1.00
SFO1         300.1318008

F2 - Processing paramete
SI                16384
SF         300.1300074
WDW                  EM
SSB                   0
LB                 1.00
GB                    0
PC                 1.00
```

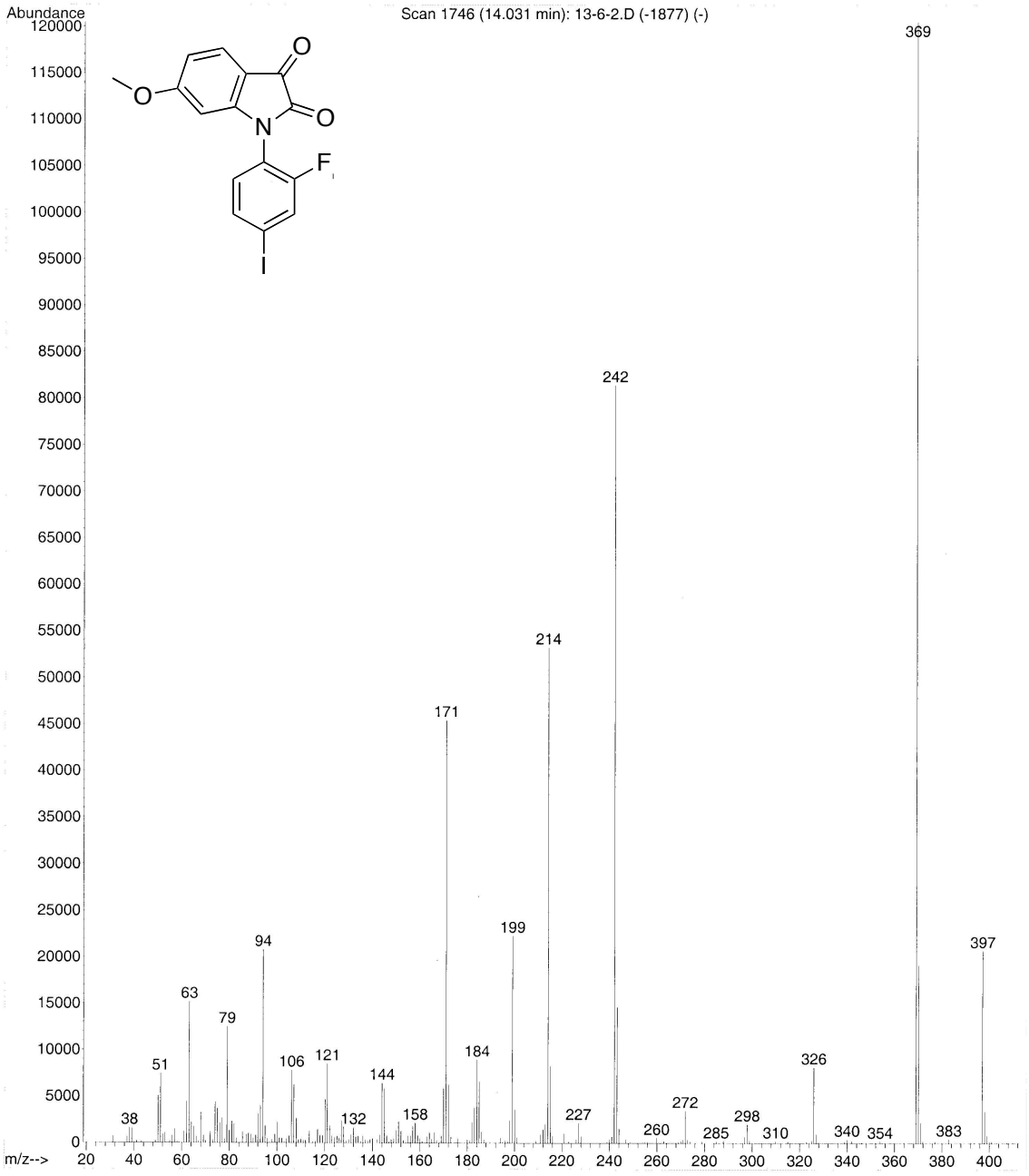
Abundance
Scan 1746 (14.031 min): 13-6-2.D (-1877) (-)
m/z-->
O
O
N
O
F
I
369
242
214
171
199
94
397
63
79
106
121
144
184
326
51
38
132
158
227
272
260
285
298
310
340
354
383

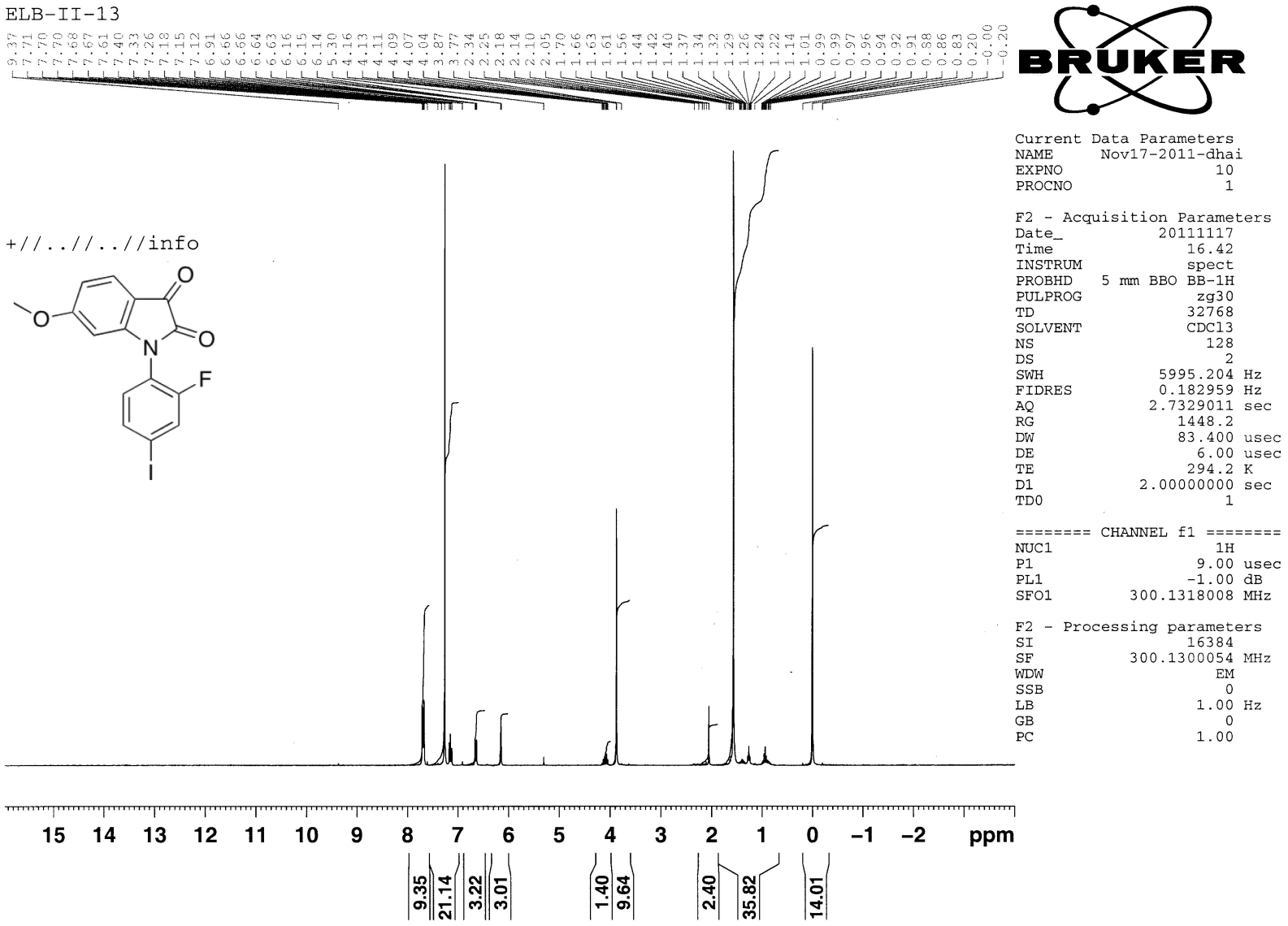

BRUKER

Current Data Parameters
NAME Nov17-2011-dhai
EXPNO 10
PROCNO 1

F2 - Acquisition Parameters
Date_ 20111117
Time 16.42
INSTRUM spect
PROBHD 5 mm BBO BB-1H
PULPROG zg30
TD 32768
SOLVENT CDCl3
NS 128
DS 2
SWH 5995.204 Hz
FIDRES 0.182959 Hz
AQ 2.7329011 sec
RG 1448.2
DW 83.400 usec
DE 6.00 usec
TE 294.2 K
D1 2.00000000 sec
TD0 1

======== CHANNEL f1 ========
NUC1 1H
P1 9.00 usec
PL1 -1.00 dB
SFO1 300.1318008 MHz

F2 - Processing parameters
SI 16384
SF 300.1300054 MHz
WDW EM
SSB 0
LB 1.00 Hz
GB 0
PC 1.00

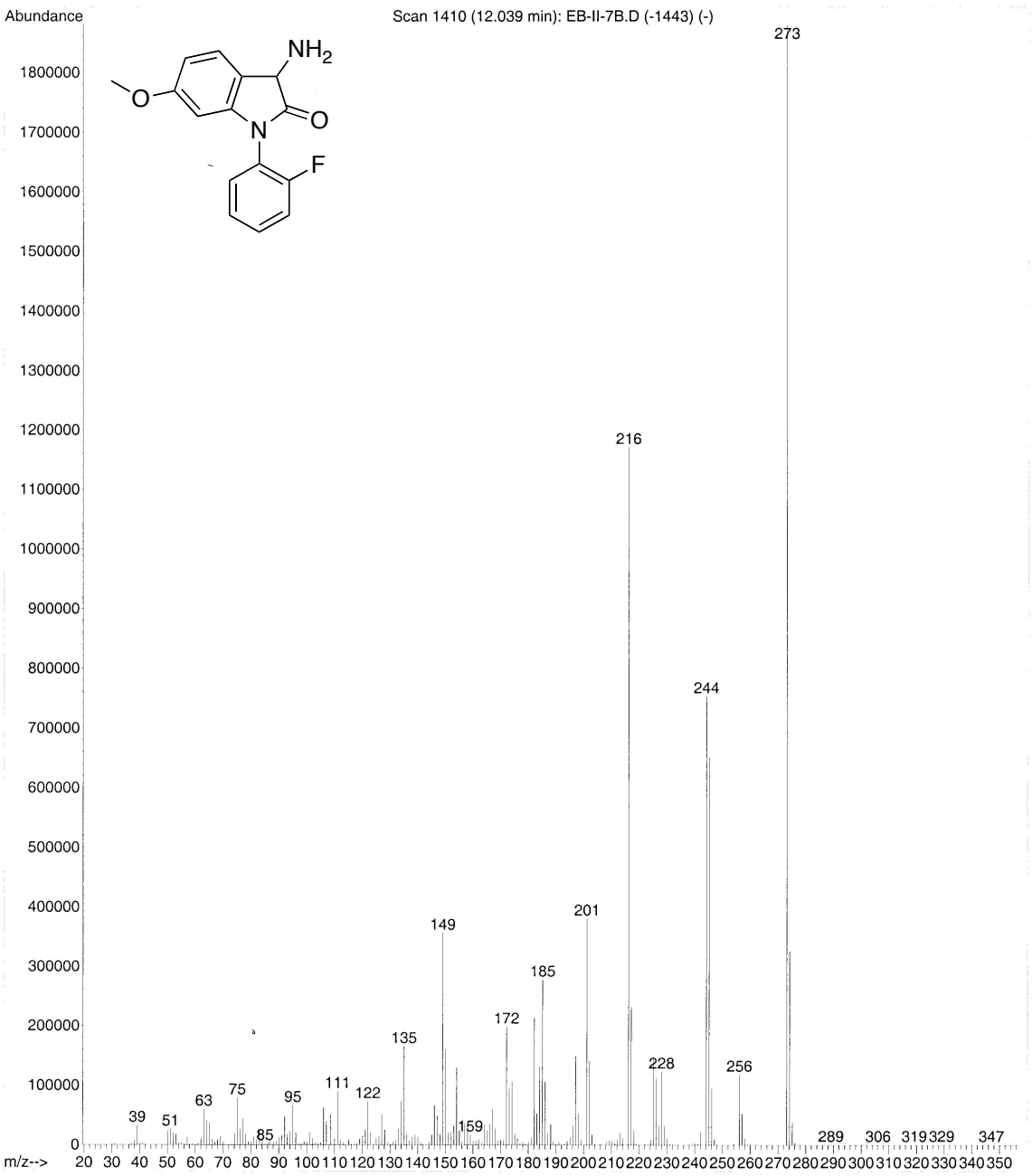
Abundance
Scan 1410 (12.039 min): EB-II-7B.D (-1443) (-)
NH2
O
N
O
F
1800000
1700000
1600000
1500000
1400000
1300000
1200000
1100000
1000000
900000
800000
700000
600000
500000
400000
300000
200000
100000
0
m/z-->
20 30 40 50 60 70 80 90 100 110 120 130 140 150 160 170 180 190 200 210 220 230 240 250 260 270 280 290 300 310 320 330 340 350
273
216
244
201
149
185
172
135
228
256
111
122
75
95
63
39
51
85
159
289
306
319
329
347

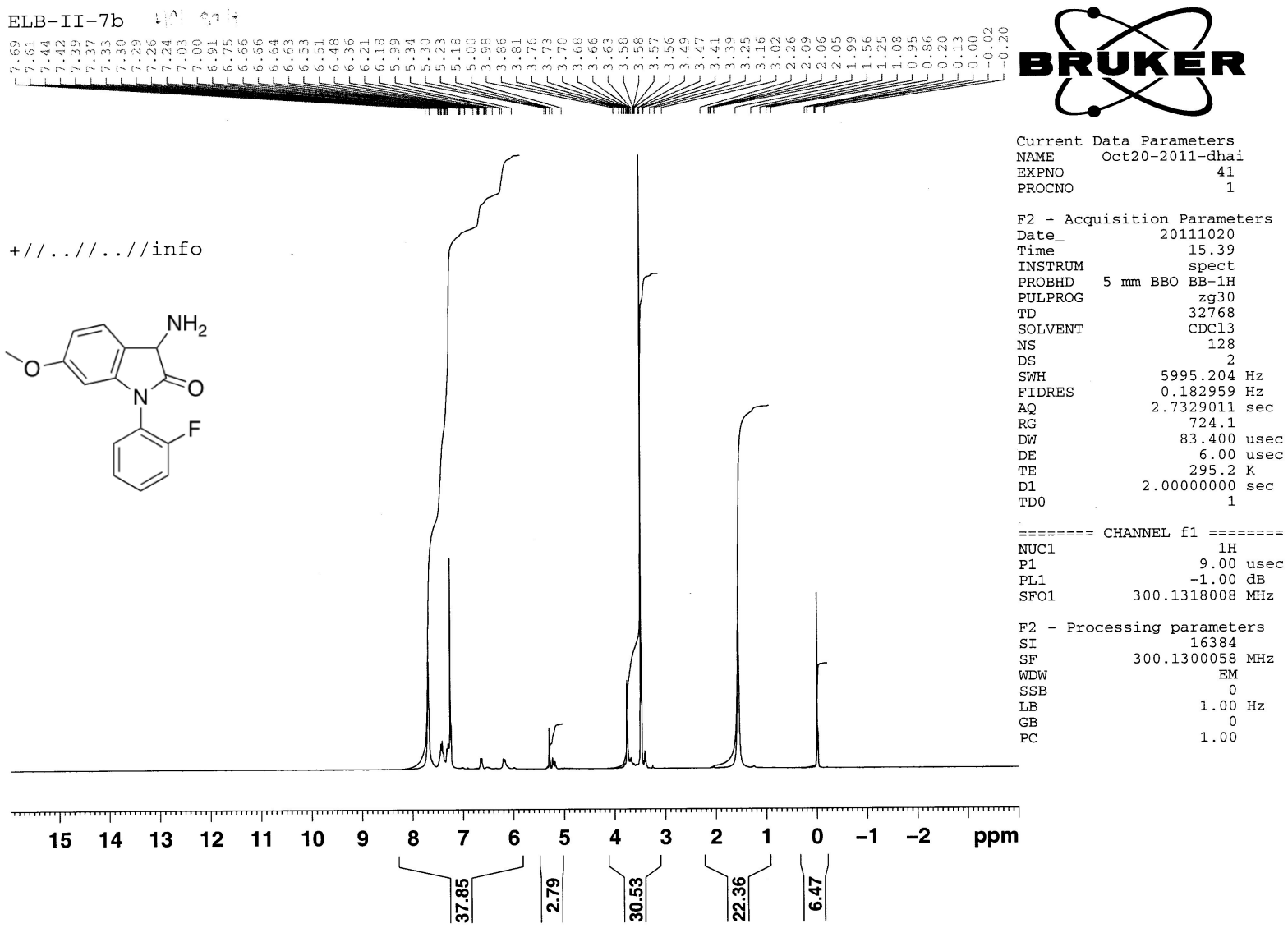

BRUKER

Current Data Parameters
NAME Oct20-2011-dhai
EXPNO 41
PROCNO 1

F2 - Acquisition Parameters
Date_ 20111020
Time 15.39
INSTRUM spect
PROBHD 5 mm BBO BB-1H
PULPROG zg30
TD 32768
SOLVENT CDCl3
NS 128
DS 2
SWH 5995.204 Hz
FIDRES 0.182959 Hz
AQ 2.7329011 sec
RG 724.1
DW 83.400 usec
DE 6.00 usec
TE 295.2 K
D1 2.00000000 sec
TD0 1

======== CHANNEL f1 ========
NUC1 1H
P1 9.00 usec
PL1 -1.00 dB
SFO1 300.1318008 MHz

F2 - Processing parameters
SI 16384
SF 300.1300058 MHz
WDW EM
SSB 0
LB 1.00 Hz
GB 0
PC 1.00

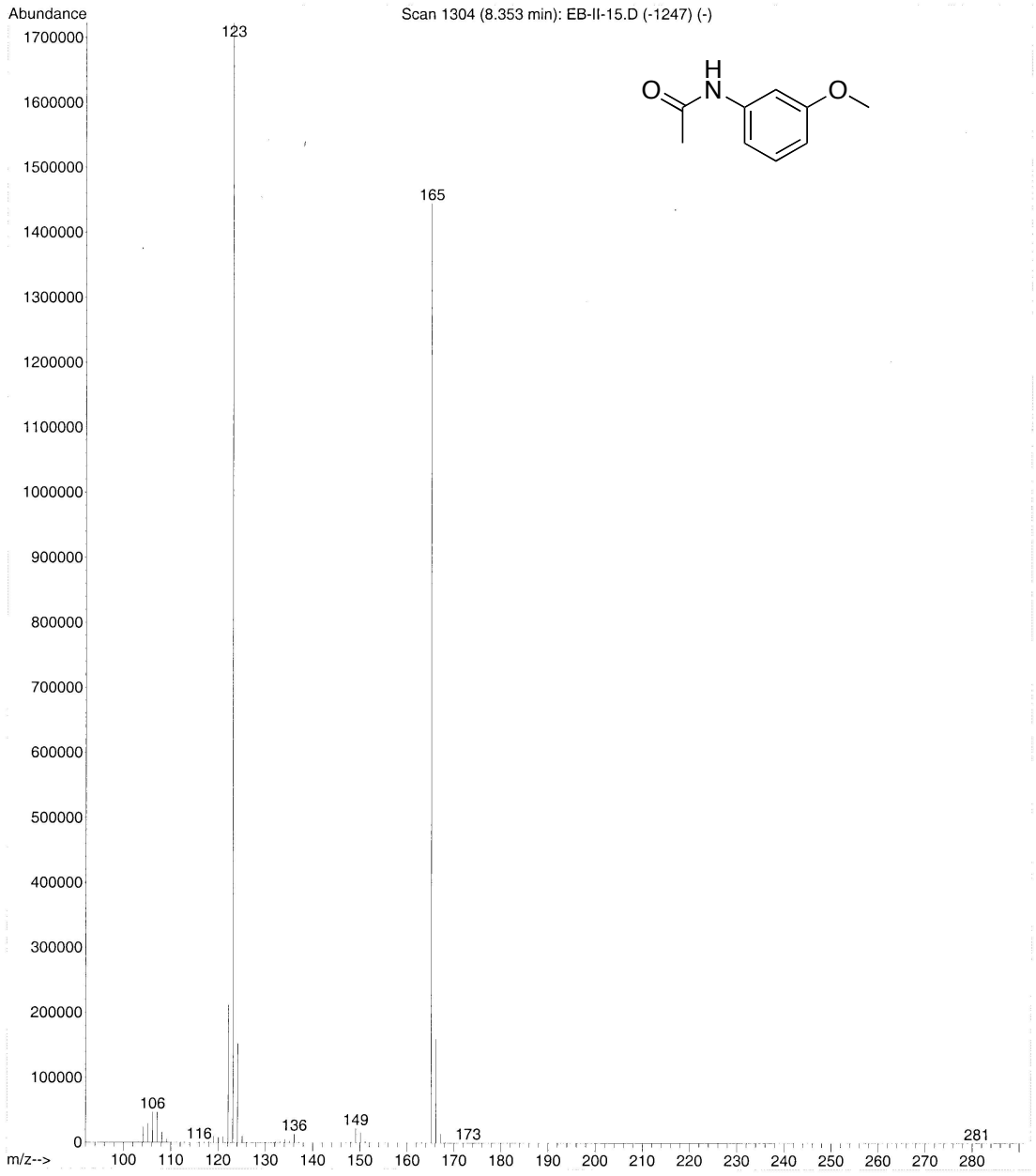
Abundance
Scan 1304 (8.353 min): EB-II-15.D (-1247) (-)
1700000
1600000
1500000
1400000
1300000
1200000
1100000
1000000
900000
800000
700000
600000
500000
400000
300000
200000
100000
0
m/z-->
100 110 120 130 140 150 160 170 180 190 200 210 220 230 240 250 260 270 280
123
165
106
116
136
149
173
281
O
H
N
O

ELB-II-15

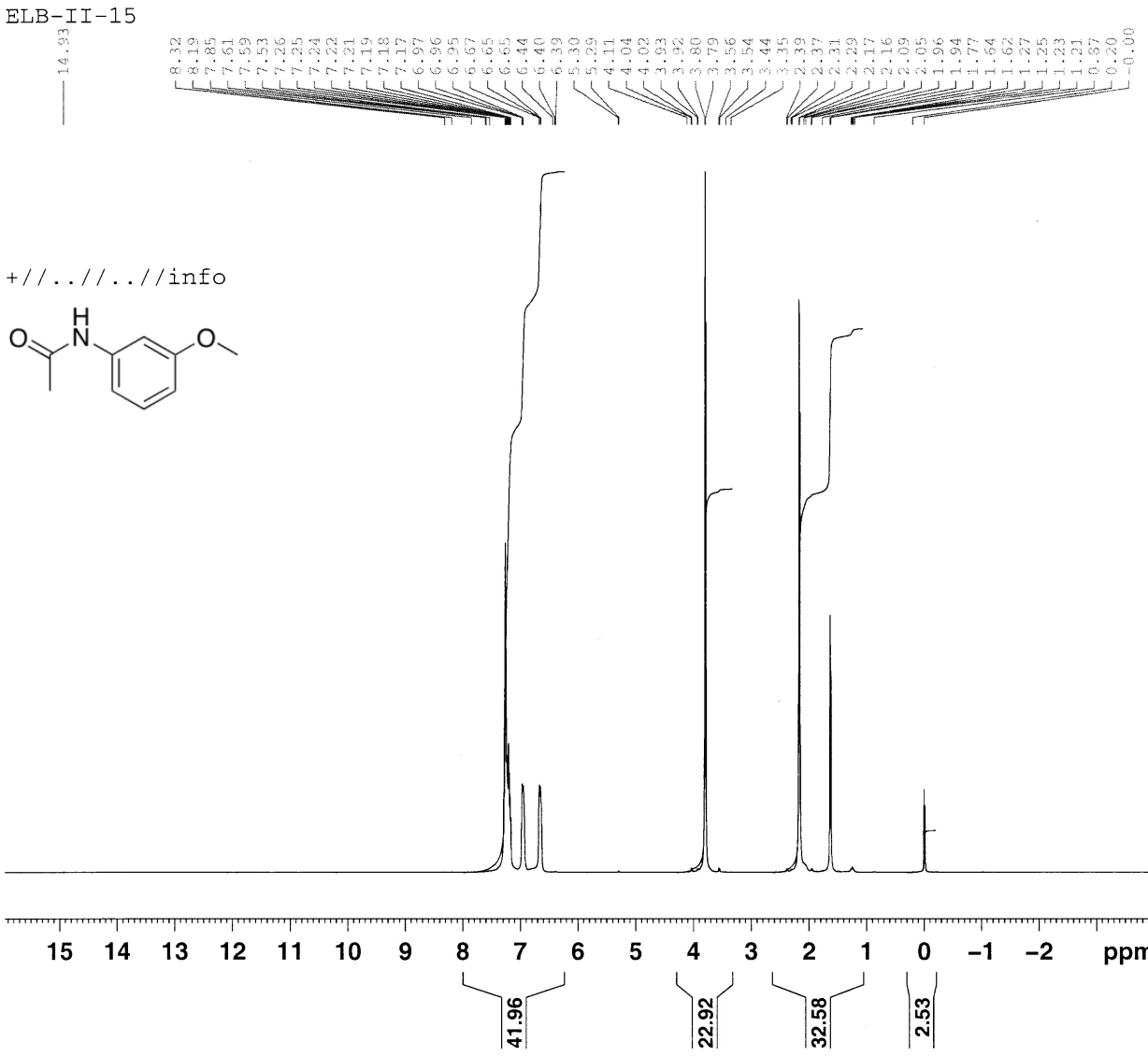

BRUKER

Current Data Parameters
NAME Jan03-2012-dhai
EXPNO 10
PROCNO 1

F2 - Acquisition Parameters
Date_ 20120103
Time 12.55
INSTRUM spect
PROBHD 5 mm BBO BB-1H
PULPROG zg30
TD 32768
SOLVENT CDCl3
NS 128
DS 2
SWH 5995.204 Hz
FIDRES 0.182959 Hz
AQ 2.7329011 sec
RG 645.1
DW 83.400 usec
DE 6.00 usec
TE 292.2 K
D1 2.00000000 sec
TD0 1

======== CHANNEL f1 ========
NUC1 1H
P1 9.00 usec
PL1 -1.00 dB
SFO1 300.1318008 MHz

F2 - Processing parameters
SI 16384
SF 300.1300089 MHz
WDW EM
SSB 0
LB 1.00 Hz
GB 0
PC 1.00